

**Interstitial diffusion from the weld metal into  
the high temperature heat affected zone in 11-  
12% chromium steel welded joints**

**By**

**ARNOLD MATTHYS MEYER**

**SUBMITTED AS PART OF THE REQUIREMENTS FOR  
THE DEGREE MASTERS IN ENGINEERING IN THE  
FACULTY OF ENGINEERING, UNIVERSITY OF  
PRETORIA**

**2000**

**Titel:** Interstisiële diffusie vanaf die sweismetaal na die hoë temperatuur  
hitte-invloedsone in 11 –12% chroomstaal sweislasse  
deur ARNOLD MATTHYS MEYER

**Leier:** M. du Toit  
Senior Lektor

**Mede-leier:** Professor G.T. van Rooyen

**Departement:** Materiaalkunde en Metallurgiese Ingenieurswese

**Graad:** M. Ing (Met)

### **Samevatting**

Kommer oor ferrietkorrelgroeï in die hitte-invloedsone van sweise in ferritiese roesvrye staal is ook van toepassing op sweise in 3CR12. Korrelgroeï beïnvloed die slageienskappe van sweislasse in 3CR12 nadelig.

‘n Hoër fraksie korrelgrensausteniet in die hitte-invloedsone van sweise in 3CR12 behoort ferrietkorrelgroeï te strem. Koolstof en stikstof is sterk austenietstabiliseerders, en behoort ‘n dubbel-fasestruktuur in die hitte-invloedsone van sweise in 3CR12 te produseer. Hierdie dubbel-fasestruktuur sou dan ferrietkorrelgroeï kon vertraag.

Hierdie werk bewys, deur berekening en eksperimentele werk, dat die fraksie austeniet in die hitte-invloedsone, die ferrietkorrelgrootte en die slageienskappe van ‘n sweislas in 3CR12, deur diffusie van koolstof en stikstof vanaf die sweismetaal na die hitte-invloedsone beïnvloed kan word.

Sweismetale met verskillende koolstofvlakke is tydens handboogsweising en gasmetaalsweising gebruik. Vervolgens is die mikrostrukture van die verskillende hitteinvloedsone ondersoek. 'n Klein ferrietkorrelgrootte is waargeneem in die hitteinvloedsone van sweislasse met 'n hoër koolstofinhoud in die sweismetaal. Verder is die slageienskappe van die sweislasse ook verbeter. Die stikstofinhoud van die sweismetaal is verhoog deur een derde stikstofgas by 'n suiwer argon skermgas te voeg, en die mengsel tydens gas-metaalsweising as skermgas te gebruik. Hierdie sweise het eweneens kleiner ferrietkorrels in die hitteinvloedsone gehad. Chemiese analise het laat blyk dat die koolstof- en stikstofinhoud van die hitteinvloedsone wel verhoog het. Die resultaat kan egter nie as finale bewys beskou word nie, aangesien die toetsmonster moontlik deur die sweismetaal besoedel kon wees.

**Title:** Interstitial diffusion from the weld metal into the high temperature heat affected zone in 11-12% chromium steel welded joints

by ARNOLD MATTHYS MEYER

**Leader:** M. du Toit  
Senior Lecturer

**Co-leader:** Professor G.T. van Rooyen

**Department:** Materials Science and Metallurgical Engineering

**Degree:** M. Eng (Met)

### **Synopsis**

Concerns regarding the grain growth in the heat-affected zones of welds in ferritic stainless steels also apply to 3CR12. Ferrite grain growth has a detrimental effect on the impact properties of welds in 3CR12.

A higher fraction of grain boundary austenite in the heat-affected zone of a weld in 3CR12 should inhibit ferrite grain growth. Carbon and nitrogen are strong austenite stabilisers and should produce a dual phase in the heat-affected zone in 3CR12 welds, thereby slowing ferrite grain growth.

This thesis shows, through calculation and experimentation, that the fraction of austenite in the heat affected zone, the ferrite grain size and the impact properties of welds in 3CR12 can be influenced by diffusion of carbon and nitrogen from the weld metal, across the fusion line into the heat-affected zone.

Weld metals with different carbon contents were used in shielded metal arc welding and gas metal arc welding. The microstructures of the heat-affected zones of the

different welds were examined. The ferrite grain sizes in the heat-affected zones of the higher carbon welds were smaller than in the lower carbon welds. Furthermore, the impact properties of the welds with the higher carbon filler metal were improved. The nitrogen content of the weld metal was increased by adding one third of nitrogen gas to a pure argon shielding gas during gas metal arc welding. The heat-affected zone grain size of these welds was smaller. Chemical analysis seemed to confirm that diffusion of carbon and nitrogen across the fusion line occurred. Results were however not conclusive because of possible contamination of the test samples by the weld metal, as the high temperature heat affected zone is very narrow and samples were obtained by drilling.

## TABLE OF CONTENTS

CHAPTER 1: Overview.....	1
CHAPTER 2: The welding of 12% chromium ferritic steels.....	4
2.1 Introduction.....	4
2.2 The welding of 3CR12.....	5
2.3 Summary.....	11
2.4 References.....	14
CHAPTER 3: The notch toughness of welded 3CR12.....	15
3.1 Introduction.....	15
3.2 The low occurrence of in service brittle failure.....	16
3.3 The heat-affected zone toughness in welded 3CR12.....	19
3.4 Summary.....	24
3.5 References.....	25
CHAPTER 4: The influence of interstitial carbon and nitrogen diffusion through the fusion line on the high temperature heat-affected zone.....	26
4.1 Introduction.....	26
4.2 The diffusion of carbon and nitrogen into the heat affected zone.....	32
4.3 Experimental welds and results.....	40
4.4 Post-weld heat treatment.....	55
4.5 Continuous cooling and diffusion.....	60
4.6 Conclusions.....	61
4.7 References.....	63

# CHAPTER 1

## Overview

The past few years have witnessed increasing interest in the use of 11% to 12% chromium steels as construction material in the transport, mining and agricultural

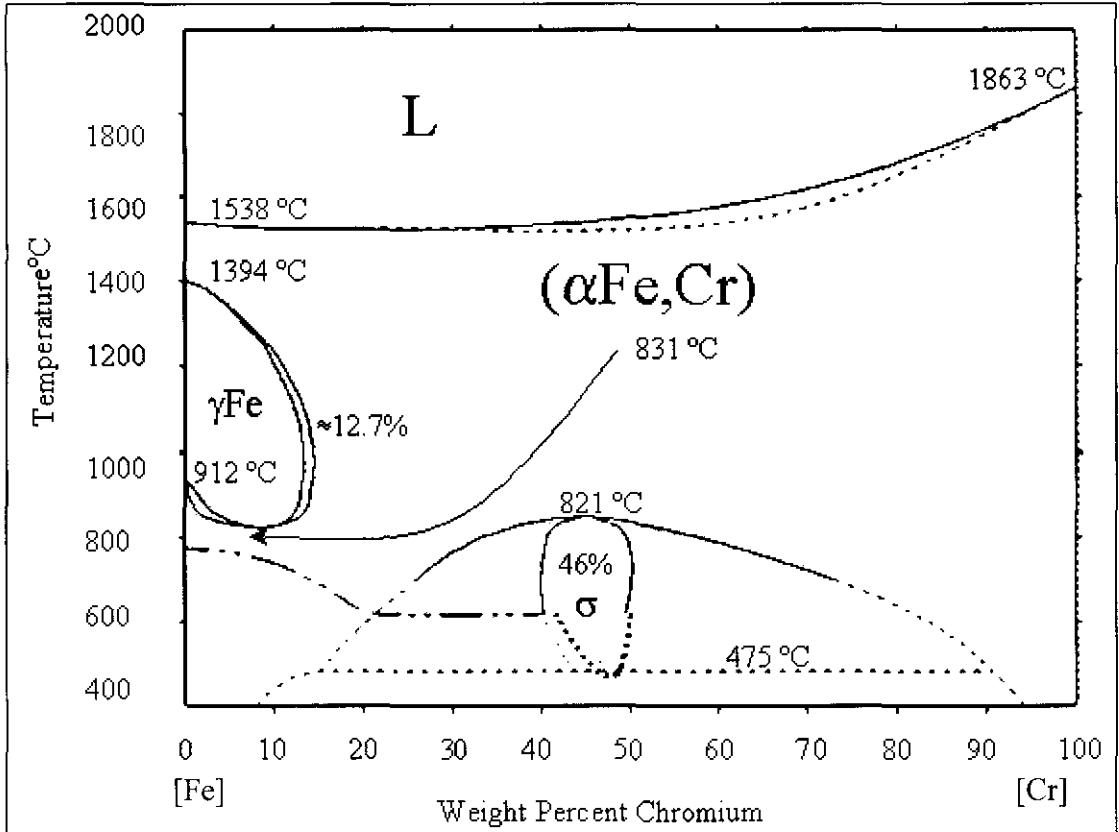


Figure 1.1: The iron-chromium equilibrium diagram<sup>5</sup>

industries<sup>1</sup>. The attraction of these steels lies mainly in the resistance offered to atmospheric corrosion. Wider acceptance has however been limited by certain potential problems associated with the welding of conventional 11-12% chromium duplex martensitic-ferritic stainless steels. Delta ferrite grain growth, with subsequent embrittlement and loss of strength, has been observed in the high temperature heat affected zone adjacent to welds in these steels<sup>2,3,4</sup>.

The possible problems associated with the welding of 11-12% chromium steels could be overcome by raising the amount of austenite formers in the steel in order to enlarge

the duplex austenite-ferrite region at high temperatures (see figure 1.1). Unfortunately, this approach would necessitate costly and time consuming alloy development, lead to increases in production costs and most probably cause an alteration in the properties obtained due to the duplex nature of the steels<sup>1</sup>. A possible alternative would be to increase the amount of austenite formers during welding in order to obtain a duplex structure in the heat affected zone at elevated temperatures. Interstitial diffusion of small austenite forming atoms such as carbon or nitrogen into the heat affected zone may be a way of promoting dual phase austenite-ferrite structure at high temperatures. In a dual phase structure the austenite on the ferrite grain boundaries effectively arrests ferrite grain growth. The carbon or nitrogen content (or both) of the heat affected zone may typically be inflated locally by diffusion from the weld metal during welding, as the atoms of both these elements are small and diffuse rapidly by interstitial migration. The high temperatures and typical thermal cycles encountered during welding suggest that this approach may have some merit, and that the microstructure of the heat affected zone may be altered in this manner (see Chapter 3).

In order to raise the interstitial carbon and nitrogen content of the heat affected zone by diffusion from the weld metal, the interstitial content of the weld metal must be raised as a pre-condition. This increase will have some practical implications. In the first place, the hardness of the weld metal will increase due to the higher levels of interstitial solute atoms. This could affect the overall behaviour of the weld under impact conditions as well as during slow loading (see chapter 3 and 4). Secondly, because of the higher carbon content of the weld metal, the corrosion resistance of the welded joint may be affected, and sensitizing would be more likely to occur. In spite of these anticipated limitations, an investigation into the feasibility of altering the phase composition of the heat-affected zone by diffusion was carried out in this study.



## 1.1. References

1. New products and applications; Columbus Stainless Steel; 7th Edition; pp. 14-19.
2. Zaayman, J.J.J; Improvements to the toughness of the heat affected zone in welds of 11 to 12 % chromium steels; PhD (UP); 1994; pp. 76-93.
3. Gooch, T.G and Ginn, B.J.; Heat affected zone toughness of MMA welded 12% Cr martensitic- ferritic steels; Report from the co-operative research programme; July 1988; pp.3-30.
4. Grobler, C; Weldability studies on 12% and 14% chromium steels; PhD (UP); 1987; pp.62-79 & 86-122.
5. Massalski, T.B.; Binary alloy phase diagrams Volume 1; American Society for Metals; Ohio; p. 866.

## CHAPTER 2

### The welding of 12% chromium ferritic steels

#### 2.1 Introduction

The majority of structural steels used today require some or other form of protection against corrosion<sup>1</sup>, such as painting or galvanizing. In order to address the need for a more corrosion resistant structural steel, Columbus Stainless has been producing a duplex ferritic/martensitic steel (3CR12) for a number of years. As shown in table 2.1, the steel contains 11% to 12% chromium, and consequently exhibits relatively good corrosion resistance over a wide range of atmospheric and aqueous conditions.

Table 2.1: The chemical composition of 3CR12. (Percentage by weight, balance Fe)

C	Ni	Mn	Si	P	S	Cr
0.03	1.50	1.50	1.00	0.03	0.03	11.0 –
max	max	max	max	max	max	12.0

3CR12 is not a stainless steel, but the rate of metal loss due to corrosion is very low. As a result, the need for expensive coatings in structural applications is diminished<sup>1</sup>. Typically, 3CR12 finds application in motor vehicles, mine ore carts and chutes handling wet farm produce<sup>1</sup>.

An apparent limitation to the general application of 3CR12 is its weldability; particularly the reduced toughness in the high temperature heat affected zone adjacent to the weld. This loss in toughness is caused by excessive delta ferrite grain growth in this area<sup>2</sup>.

A number of studies have shown that acceptable impact strengths in the welded joint can be obtained when 3CR12 is welded using an austenitic filler metal such as 309 or 309L<sup>3,4</sup>. However, ferrite grain growth in the heat affected zone cannot be prevented

and this still presents problems when plate thicker than 3mm is welded. It is not critical for general thin plate applications, and ideally 3CR12 could be used in applications reserved traditionally for carbon steels, such as AISI 1010 used in the transport industry<sup>5</sup>.

The heat affected zone properties of 3CR12 welds may be improved if grain growth in the high temperature heat affected zone can be prevented or at least restricted. Ferrite grain growth can be reduced by balancing the chemical composition of the parent metal to include more austenite forming elements<sup>3</sup>, but the cost of these additions would increase the price of the steel. The aim of this study was to investigate the potential for raising the local interstitial carbon and/or nitrogen content of the high temperature heat affected zone by diffusion over the fusion line, and thereby stabilizing the austenite ( $\gamma$ ) phase locally. The increased stability of the austenite should give rise to a dual phase structure (consisting of ferrite and austenite) at high temperature, and may restrict  $\delta$ -ferrite grain growth. This chapter discusses current practices of welding 3CR12, and the typical heat affected zone microstructures that can be expected adjacent to the fusion line.

## **2.2. The Welding of 3CR12**

### **2.2.1 Welding procedures and heat input**

The shielded metal arc welding (SMAW) and the gas metal arc welding (GMAW) processes are used in practice to weld thicker sections of 3CR12 (thicker than 3mm)<sup>1</sup>. Plate sections thinner than 3mm are usually welded with gas tungsten arc welding (GTAW)<sup>1</sup>. Submerged arc welding can be used only after extensive procedure testing, as the high heat input and slow cooling rates associated with this process can cause loss of toughness in the heat affected zone<sup>1</sup> due to excessive ferrite grain growth. The heat input should be kept to the minimum to improve the integrity of the weld<sup>1</sup>. During SMAW a short arc length should be maintained, weaving and back stepping should be avoided to minimize the heat input, and the current should be set at the low to medium end of the range recommended by the manufacturer of the welding

electrodes<sup>1</sup>. An austenitic filler metal with a low carbon content (such as E309L) is usually recommended<sup>1</sup>.

### **2.2.2. The Heat Affected Zone in welded 3CR12 plate**

According to Grobler<sup>3</sup>, the heat affected zone in 3CR12 can be divided into three separate zones. The three zones are defined in the following way:

#### **(a) The high temperature heat affected zone (HTHAZ)**

The HTHAZ is a narrow coarse grained zone directly adjacent to the fusion line. It is heated into the  $\delta$ -ferrite phase field during welding (see figure 2.1 and 2.2), and due to the very high peak temperatures reached, excessive ferrite grain growth occurs. The final structure generally consists of  $\delta$ -ferrite with blocky Widmanstätten martensite on the grain boundaries (see figure 2.3). The fraction martensite depends not only on the relative amount of ferrite and austenite stabilizers present in the steel, but also on the rate of cooling through the austenite ( $\gamma$ ) phase field.

Typical peak temperatures reached during welding are shown graphically in figure 2.2. The curves in figure 2.2 were obtained from calculations based on the Rosenthal equation<sup>7</sup>. The Rosenthal equation, together with the relevant calculations, will be discussed in more detail in Chapter 4. The graphs were obtained on the assumption that the fusion line peak temperature is equal to the liquidus temperature of 3CR12. The liquidus temperature was estimated from the phase diagram (figure 2.1) to be approximately 1510 °C. The distance from the center of the heat source to the fusion line can then be measured, and the temperature sequence for a point at this distance from the fusion line can be calculated. The results indicate that the large delta ferrite grains form at a temperature above a certain peak temperature at a specific distance away from the fusion line. The width of the heat affected zone can be observed and measured by applying a light etch with Kalling's no. 2 reagent, and was found to be 0.5mm for the conditions in figure 2.2.

Grain boundary austenite formed during the heating cycle effectively inhibits grain growth, and transforms to martensite on cooling. During cooling, some of the  $\delta$ -ferrite transforms to grain boundary austenite. In the case of a HTHAZ with no austenite on the ferrite grain boundaries, the composition of the heat lies to the extreme right of the dual phase austenite and ferrite region in the iron-chromium phase diagram (figure 2.1). As a result the time available for austenite formation is limited during the heating and cooling cycles<sup>4</sup>. The width of the HTHAZ depends on the heat input and the chemistry of the specific heat, and varies between 0,1 mm and 0,5 mm<sup>4</sup>. Thermal cycle predictions with the Rosenthal equation can be used to predict the width of the HTHAZ. (See chapter 4).

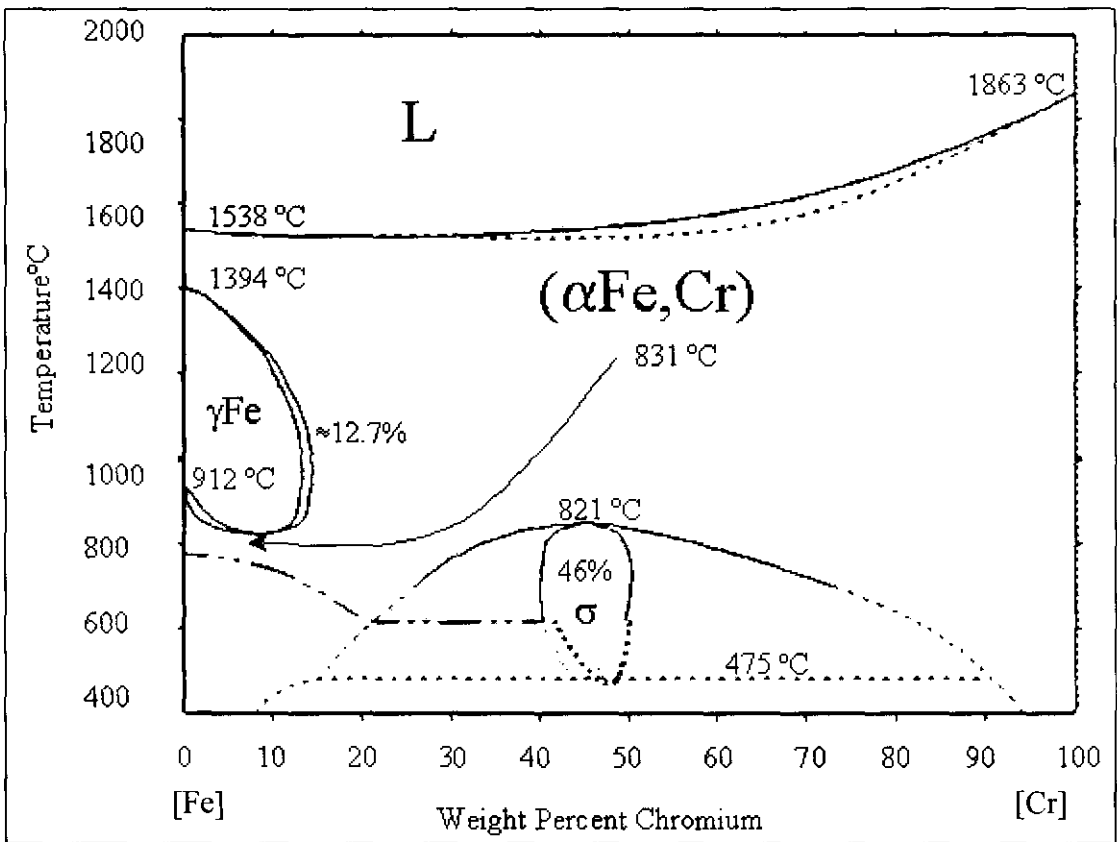


Figure 2.1: The iron-chromium equilibrium diagram

**b) The duplex zone**

A much wider duplex zone is located adjacent to the HTHAZ. This zone consists of fine grained ferrite and untempered intergranular and transgranular martensite (figure 2.4). This zone originated when the steel was heated into the dual phase (austenite + ferrite) phase field in figure 2.1. The phase composition of the duplex zone varies

across the width of the zone. As discussed earlier the high temperature heat affected zone adjacent to the fusion line consists of large delta ferrite grains with blocky martensite on the grain boundaries. Within the duplex zone the fraction martensite increases with distance from the fusion line, while the delta ferrite grains become smaller. The ferrite grains tend to be elongated further away from the fusion line. The width of the duplex zone is dependent on both the individual heat composition and the heat input during welding. This zone exhibits a high hardness, mainly because of the high fraction of untempered martensite present in the microstructure

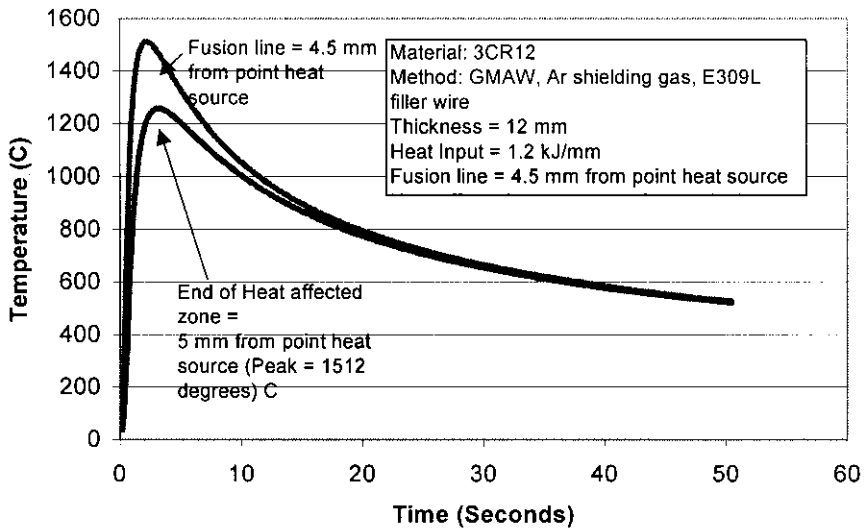
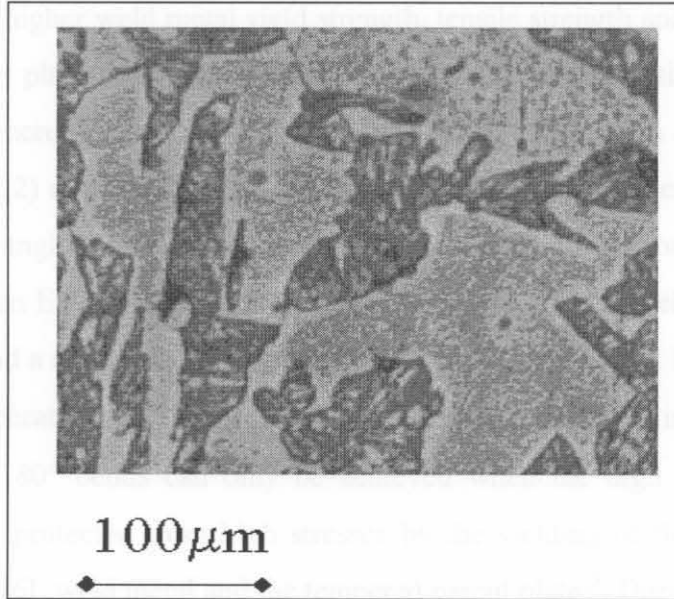


Figure 2.2: The welding temperature sequence from Rosenthal<sup>7</sup>.

**(c) The low temperature heat affected zone.**

The low temperature heat affected zone is more distant from the fusion line, and was heated to below the transition temperature to the dual phase (austenite + ferrite) region (see figure 2.1) during welding. The hardness of the parent plate remains unchanged in this zone<sup>3</sup>. The steel exhibits a relatively high tempering resistance, and the time at

high temperature is too short for any additional tempering to occur<sup>6</sup>. The low temperature heat affected zone does not exhibit significant metallurgical changes during welding<sup>3</sup>.



**Figure 2.3:** The high temperature heat affected zone.(GMAW, HI=1.3kJ/mm, etched by quick swabbing with Kalling's reagent nr.2<sup>8</sup>).

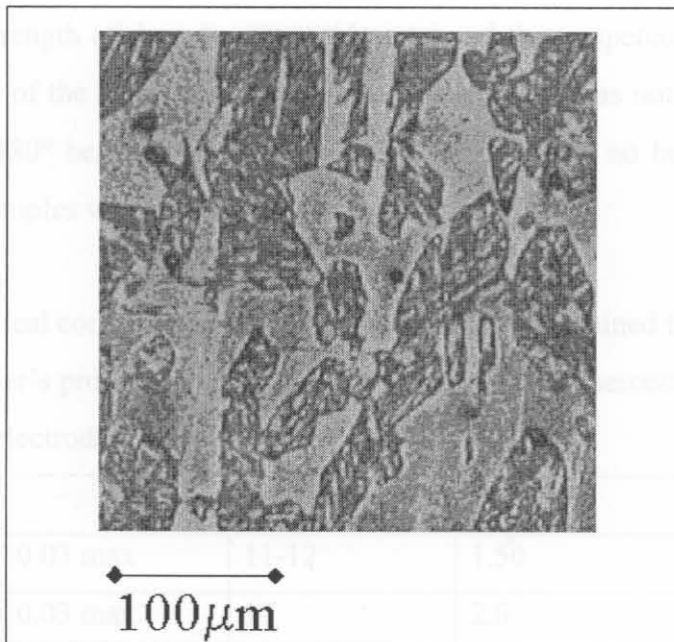


**Figure 2.4:** The duplex zone. (GMAW, HI = 1.3 kJ/mm, etched by quick swabbing with Kalling's

### 2.2.3 Filler Metals for welding 3CR12

Generally, the susceptibility to brittle fracture in the HTHAZ in 3CR12 welds increases with a higher weld metal yield strength, tensile strength and work hardening rate<sup>3</sup>. In bead on plate bend tests performed by Grobler<sup>3</sup>, the maximum bend angle decreased with increasing weld metal hardness. An E3CR12 (with a composition as shown in table 2.2) electrode yielded the highest weld metal hardness, but the lowest maximum bend angle. The bend angle obtained from the E3CR12 welded plates was only 13°. With an E316L electrode (see table 2.2) a much lower weld metal hardness was obtained, and a maximum bend angle of 180° could be reached. Fracture occurred in the high temperature heat affected zone adjacent to the fusion line. This suggests that successful 180° bends can only be achieved when the high temperature heat affected zone is protected from high stresses by the yielding of the adjacent softer material (the E316L weld metal and the tempered parent plate)<sup>3</sup>. During bending, most of the deformation in the specimens welded with the E316L occurred in the low strength low temperature heat affected zone, with some deformation in the weld metal, and almost none in the high temperature coarse grained zone<sup>3</sup>. As a result of the relatively low strength of the adjacent weld metal and the tempered parent plate, the fracture strength of the high temperature heat affected zone was not exceeded during bending<sup>3</sup>, and 180° bends could be achieved. Unfortunately, no bending tests were carried out on samples welded with E309L electrodes.

Table 2.2: Chemical composition of different electrodes as obtained from the supplier's product information. All values are mass percentages. An E307 electrode was not tested by Grobler.

<b>Electrode</b>	<b>C</b>	<b>Cr</b>	<b>Mn</b>	<b>Ni</b>
<b>E3CR12</b>	0.03 max	11-12	1.50	1.50
<b>E316L</b>	0.03 max	17	2.0	12
<b>E309L</b>	0.03 max	23	2.0	13.5
<b>E307</b>	0.16	15-17	2.0	12-13



As a rule, a 309L filler metal is recommended when welding 3CR12 for high integrity structural applications<sup>1</sup>. This austenitic type filler metal has a low yield strength relative to the 3CR12 parent plate, and consequently protects the grain growth zone against brittle fracture by absorbing a high fraction of the plastic deformation during bending<sup>3</sup>. At high dilutions (higher than 43%<sup>3</sup>) weld metal martensite forms. The yield strength of the weld metal will increase due to the presence of weld metal martensite, and this would be detrimental to the fracture toughness of the weld as the weld metal would not be able to absorb sufficient plastic deformation. As a result, the fracture strength of the high temperature heat affected zone may be exceeded during bending. The major disadvantages of the E309L filler metal are that it is relatively expensive and that the possibility of galvanic corrosion in certain environments exists<sup>3</sup>. In order to avoid galvanic corrosion and provide an electrochemical match between the weld and the parent plate, the composition of the weld has to closely resemble that of the parent plate. Such a matching electrode, for example E3CR12, would lie in the ferrite-martensite phase field on the Schaeffler diagram (figure 2.5), indicating that untempered martensite would be present in the weld metal. As a result, E3CR12 welds have high yield strengths and cannot protect the grain growth zone from brittle fracture by plastic deformation of the weld metal<sup>3</sup>. For this reason, the E3CR12 filler metal is not recommended for welding of 3CR12 in any structural type application, particularly not if the impact strength of the welded joint is critical<sup>3</sup>.

The conclusion can be drawn that neither the E309L, nor the E3CR12 filler metals, meet both the electrochemical and the mechanical requirements as filler metal for welding 3CR12<sup>3</sup>. In practice, the particular application would determine the choice between these two filler metals<sup>3</sup>, as well as between other filler metals such as E316L (See the Schaeffler diagram in figure 2.5).

## 2.3 Summary

3CR12 offers good corrosion resistance in mild environments. During the welding of thick sections of 3CR12, embrittlement of the high temperature heat affected zone may occur as a result of  $\delta$ -ferrite grain growth in the high temperature heat affected

zone adjacent to the weld. The detrimental effect of the ferrite grain growth may be reduced by welding with a relatively soft, low carbon austenitic filler metal such as E309L or E316L. Plastic deformation in the weld metal and in the parent metal protects the heat affected zone by preventing the fracture stress of the high temperature heat affected zone from being exceeded. However, the chemical compositions of E309L and E316L are notably different from that of 3CR12, and galvanic corrosion may occur if these filler metals are used in highly corrosive environments. An E3CR12 filler metal provides the electrochemical match to the parent metal to prevent galvanic corrosion, but as a result of the large quantity of untempered martensite in the weld metal, the weld will be very hard. As a result, the E3CR12 weld metal would be unable to absorb sufficient plastic deformation to protect the heat affected zone from stresses that may exceed the fracture stress of the zone.

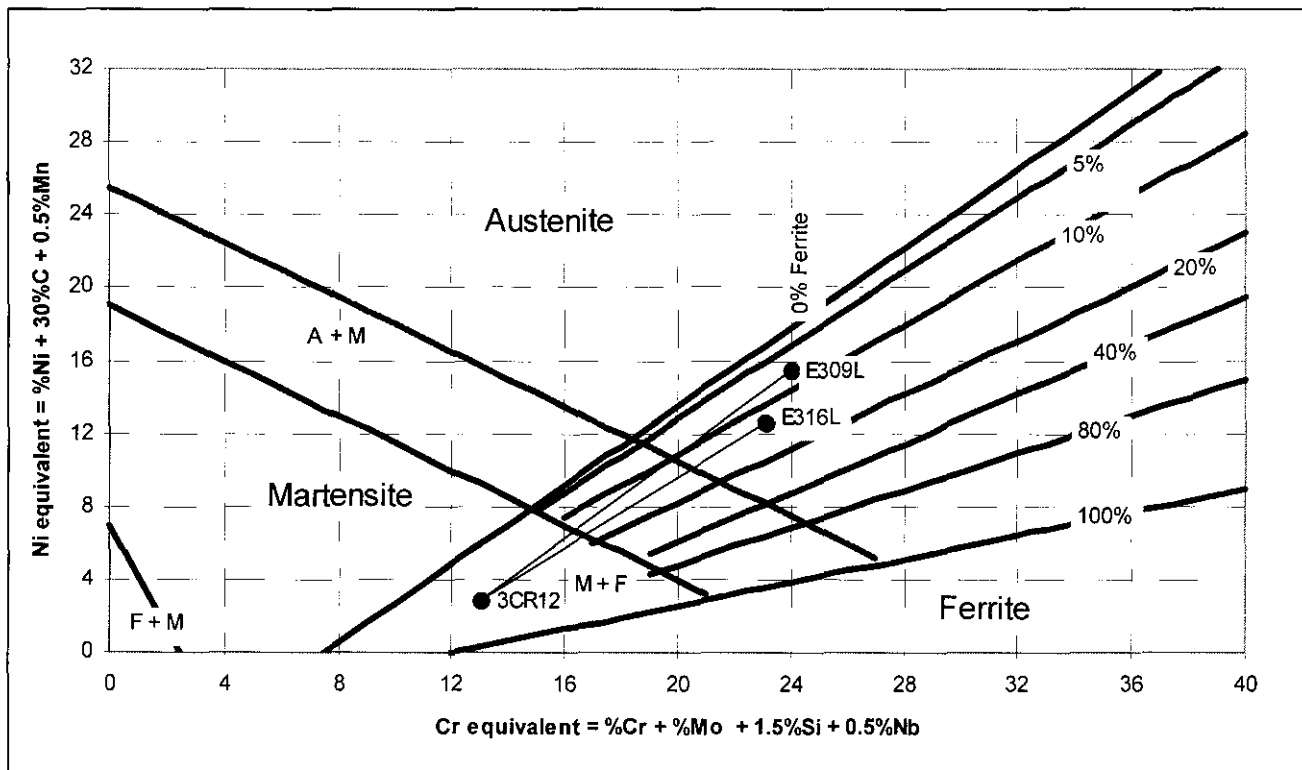


Figure 2.5: The Schaeffler diagram, showing different filler metal compositions<sup>2</sup>.

The conclusion can be drawn that the welding of 3CR12 is a compromise between the corrosion resistance and the impact strength of the welded joint. The relative importance of the two characteristics in a specific application would determine the choice of the filler metal.

## 2.4 References

1. Product Guide for 3CR12; Middelburg Steel and Alloys (Pty) Limited; January 1988; pp. 1-19
2. Gooch, T.G. & Ginn, B.J.; Heat affected zone toughness of MMA welded 12%Cr martensitic-ferritic steels; Report from the co-operative research programme for research members only; The welding institute; Cambridge; 1988; pp. 3-9.
3. Grobler, C; Weldability studies on 12% and 14 % chromium steels; Ph.D. UP (1987); pp. 23-26
4. Zaayman, J.J.J; The heat affected zone toughness of 11 to 12 per cent chromium steels; M. Eng.; UP (1992); pp 31-57.
5. Bolton, W; Engineering Materials Handbook; Butterworth-Heinemann Ltd.; Oxford; 1993; pp. 46-59.
6. Llewellyn, D.T.; Steels: Metallurgy and applications; Butterworth-Heinemann Ltd.; Oxford; Second Edition 1994; Second Impression 1995; pp.221-244.
7. Easterling, K; Introduction to the physical metallurgy of welding; Butterworth-Heinemann; Oxford; Second Edition 1992; Second Impression 1993; pp.1-38.
8. Kehl, G.L.; Principles of Metallographic Laboratory Practice; McGraw-Hill Book Company New York; Third Edition 1949; pp. 409-447.

## CHAPTER 3

### The notch toughness of welded 3CR12

#### 3.1 Introduction

Steels with 11% to 12%Cr conventionally have predominantly martensitic structures, and require preheating in order to prevent hydrogen cracking during welding. The welded joints may also require post-weld heat treatment in order to temper the transformed weld area and to improve the toughness of the joints<sup>1</sup>.

During welding, the high temperature heat affected zone (as discussed in Chapter 2) in 3CR12 is heated into the delta ferrite phase region on the iron-chromium phase diagram<sup>2</sup>. The structure consequently transforms to  $\delta$ -ferrite and massive ferrite grain growth occurs (even at low heat inputs), which can cause a major loss of toughness in the weld area<sup>1</sup>.

In spite of the above-mentioned problems, in-service brittle failures have been infrequent in welded 3CR12 components. There are a number of possible explanations as to why brittle failure in welded 3CR12 is not experienced regularly. In the first place, most commercial applications for 3CR12 employ section thicknesses of 5mm or less<sup>3</sup>, and therefore the through-thickness constraint is low. In the second instance, the grain growth region is narrow and is surrounded by 3CR12 parent plate and austenitic (usually 309L) weld metal. Both the 3CR12 and the 309L have relatively high toughness. Furthermore, the austenitic 309L does not exhibit a ductile-to-brittle transition temperature. In addition, the applied stress is often low. The service temperature is also of significant importance, and under South African conditions the service temperature may be higher than the ductile-to-brittle transition temperature of the heat affected zone, so that fracture would not occur unless severe impact loading is involved<sup>3</sup>.

## 3.2 The low occurrence of in service brittle failure

As stated above, few occurrences of in-service brittle failure of welded 3CR12 components have been reported. The main reasons for the lack of brittle failure, namely the low through-thickness constraint and the protection offered to the high temperature heat affected zone by the weld metal and parent metal will be discussed in the subsequent chapters.

### 3.2.1 Low through-thickness constraint

Through-thickness plastic constraint is one of the most important factors that may lead to brittle failure. In some cases a full sized Charpy specimen may not be a realistic model of the actual situation that would exist in thicker sections in practice<sup>4</sup>. The difference in through-thickness constraint causes a phenomenon that is illustrated in figure 3.1. The relatively small Charpy specimen does not provide the same constraint as present in a larger specimen, and at a specific service temperature the sub-thickness Charpy specimen may show high impact energy, while the same material in a standard section would have a low toughness<sup>4</sup>.

The dependence of the fracture toughness on the plate thickness can also be seen in figure 3.2. In the diagram,  $B_1$  denotes a plate thickness at which the plane strain, or normal fracture, dominates sufficiently so that the fracture toughness effectively equals  $K_{Ic}$ . At this thickness, the central normal fracture is large enough so that the shear fractures at the ends of the crack do not influence the fracture toughness<sup>5</sup>. For any thickness less than  $B_1$ , the shear fractures at the front and the back of the plate become significant factors in determining the magnitude of the fracture toughness  $K_c$ . Consequently,  $K_c$  rises at thickness values below  $B_1$  as the size of the central region undergoing plane strain decreases relative to that of the two shear lips, since the shear lip size tends to be independent of the plate thickness<sup>5</sup>. A maximum in the fracture toughness is shown at  $B_0$ , and the corresponding fracture toughness value is often used as the plane stress fracture toughness<sup>5</sup>. Below  $B_0$ , thin plates tend to exhibit simple

shear fractures<sup>5</sup>. The influence of plate thickness on the fracture toughness is well understood, and is probably one of the most important reasons for the low occurrence of brittle fractures in 3CR12 welds in practice, as 3CR12 is mostly used in plate thicknesses of 5mm or less. The fact that 3CR12 welds exhibit a low occurrence of brittle failure in practice is an important factor determining the application of the steel in the automobile industry<sup>6</sup>.

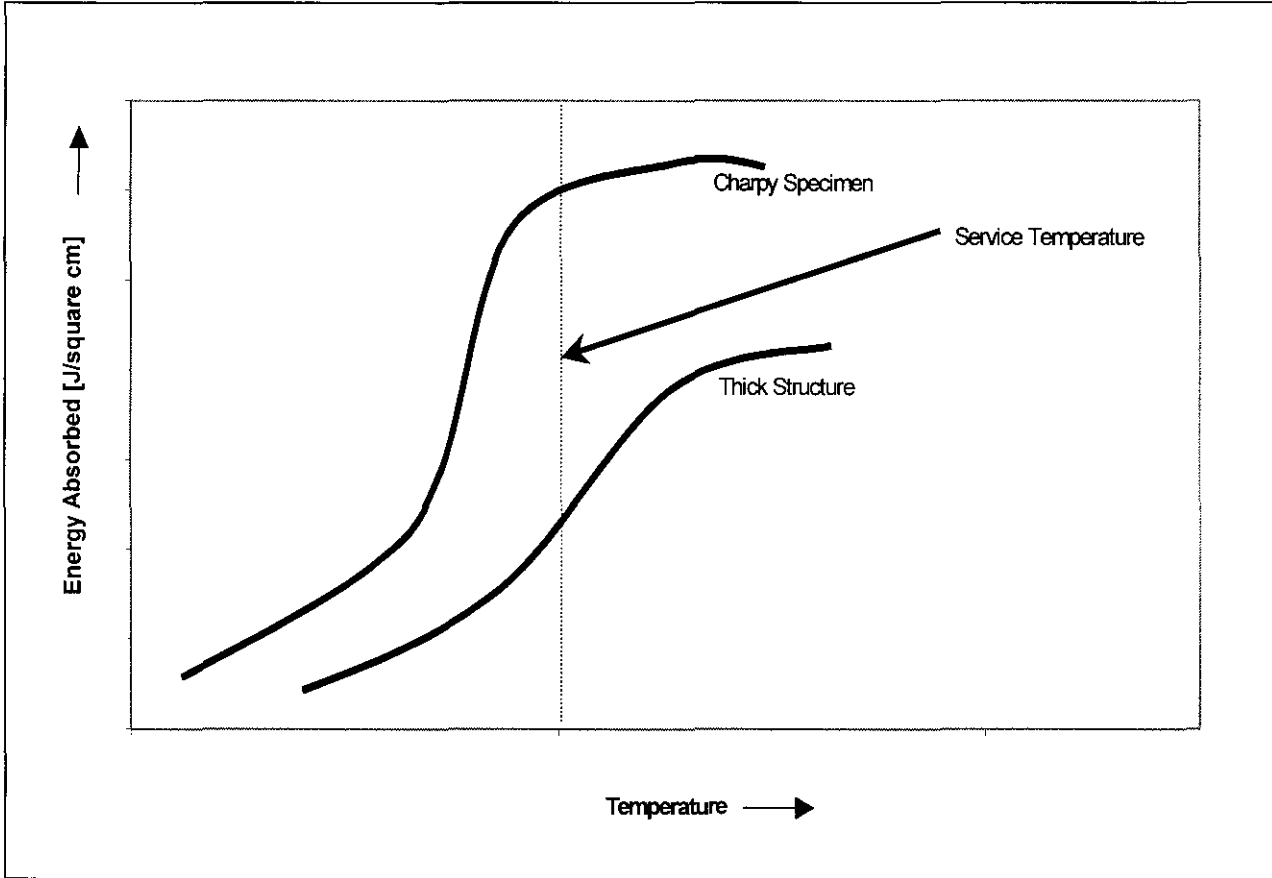


Figure 3.1: The effect of section thickness on transition temperature curves<sup>4</sup>.

### 3.2.2 The protection of the HAZ by the weld metal and the parent metal.

The use of 309L weld metal is recommended for welding 3CR12 (E316L or other austenitic consumables are sometimes also recommended) as a result of the protection offered by the relatively soft weld metal to the coarse and brittle high temperature heat affected zone. In bead-on-plate bend tests performed by Grobler<sup>7</sup>, the tendency for brittle failure in the high temperature heat affected zone increased with increasing weld metal hardness. The highest maximum bend angles were obtained when an

E309L or an E316L filler metal was used<sup>7</sup>. 180° bend angles could be obtained because almost all of the plastic deformation occurred in the relatively soft weld metal and parent metal, and consequently the fracture stress of the brittle, coarse grained high temperature heat affected zone was not exceeded<sup>7</sup>. The untempered martensite on the delta ferrite grain boundaries in the high temperature heat affected zone causes it to be harder than the surrounding parent metal and weld metal, and as a result plastic deformation tends to occur in those areas instead of in the high temperature heat affected zone during bending<sup>7</sup>. The conclusion can be drawn that an increase in the relative hardness of the heat-affected zone could have a positive effect on the impact properties of the joint.

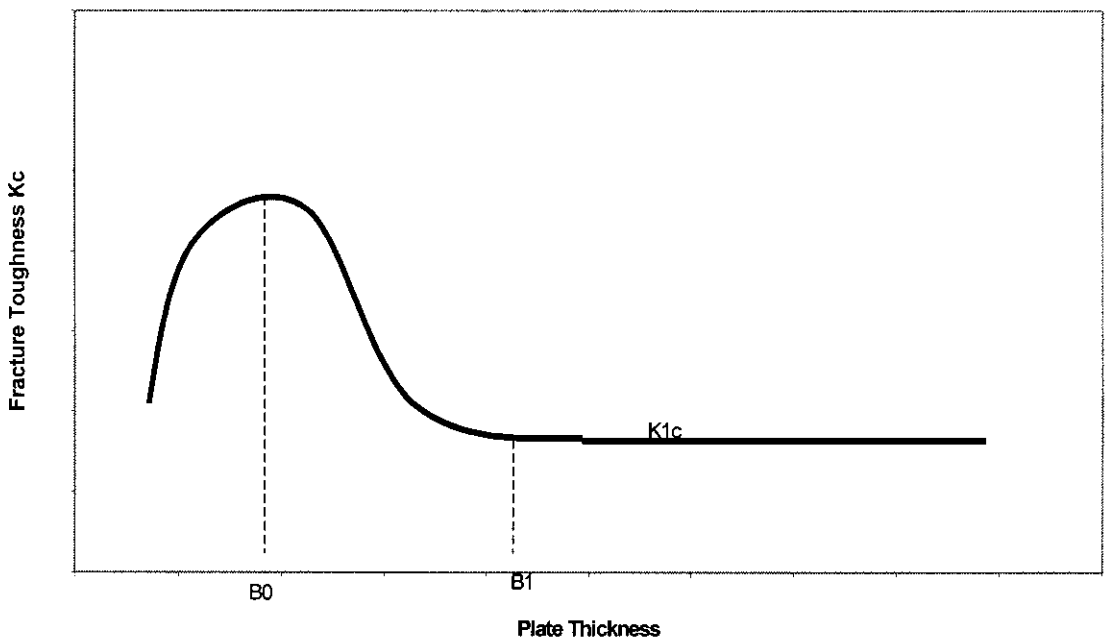


Figure 3.2: The dependence of the fracture toughness on the plate thickness<sup>5</sup>.



### **3.2.3 The orientation of the heat affected zone relative to the applied impact load.**

The orientation and shape of the HAZ relative to the applied impact load have a major influence on the energy absorbed during the Charpy test. The narrow width of the grain growth zone (200  $\mu\text{m}$  max) makes it very difficult to place the tip of a Charpy notch directly into the grain growth zone. The contour which the fusion line and the high temperature heat affected zone follows through the thickness of the plate is also important. If the grain growth zone has a curved or a K-type form (see figure 3.3), the placement of the notch tip directly into the grain growth zone becomes even more difficult. In order to obtain a grain growth zone that runs straight through the thickness of the Charpy specimen, a butter layer was welded on the flat side of a K-type weld preparation for the purpose of the experiments (see figure 3.3). If this type of preparation is not used, the crack will propagate into the parent metal or the weld metal, and the true properties of the grain growth zone will not be determined in the Charpy test. Even with this preparation, the precise placement of the notch tip into the grain growth zone is still difficult, and a large number of weld metal and parent metal failures occur<sup>2</sup>. Properly prepared (such as a double V-type or a K-type without a butter layer) welded structures in practice would render straight crack propagation through the grain growth zone difficult if not impossible, and would contribute to the fact that brittle failure in the heat affected zone of 3CR12 rarely occurs in service. The difference between a prepared butter layer K-type joint for the Charpy impact test and a practical double V-type preparation is shown in figure 3.3.

### **3.3 The heat affected zone toughness in welded 3CR12**

As mentioned earlier, excessive  $\delta$ -ferrite grain growth occurs in the high temperature heat affected zone in welded 3CR12. The grain growth is detrimental to the impact strength of the heat-affected zone. Although few brittle failures of 3CR12 welds have been reported, the observed ferrite grain growth nevertheless causes concern about the impact properties of welds in 3CR12, as the effect of grain size on impact resistance is well known and well documented. The theoretical influence of grain size is discussed in the following paragraphs.

Cottrell discussed the important variables that play a role in brittle fracture<sup>4</sup> and derived an equation that provides the limiting condition for a crack to form and propagate:

$$(\tau_i d^{1/2} + k')k' = G\gamma_s\beta \quad \dots\dots\dots (3.1)$$

where  $\tau_i$  = the resistance of the lattice to dislocation movement

$k'$  = a parameter related to the release of dislocations from a pile up

$\gamma_s$  = the effective surface energy + the energy of plastic deformation

$d$  = grain diameter

$\beta$  = a term which expresses the ratio of shear stress to normal stress. For

torsion  $\beta = 1$ ; for tension  $\beta = 1/2$ ; for a notch  $\beta = 1/3$ .

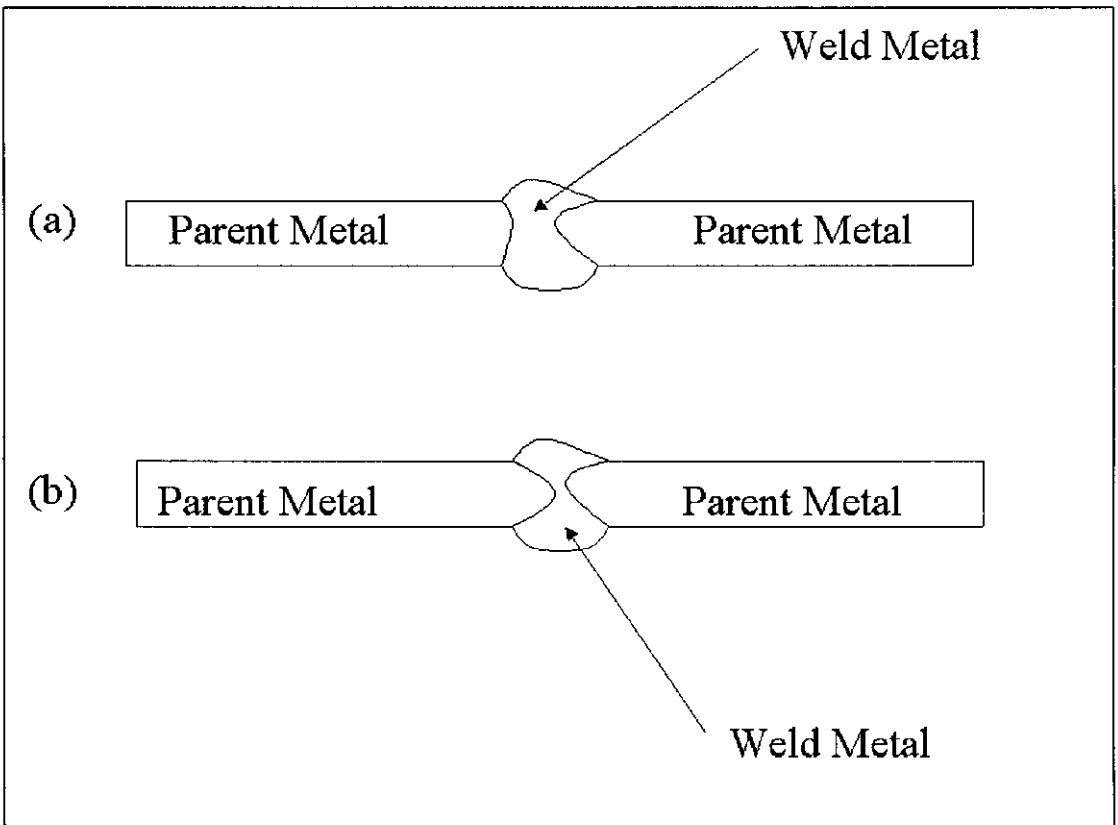


Figure 3.3: a) A butter layer K-type preparation b) A double V-type preparation.

If the left side of equation (3.1) is smaller than the right side, microcracks can form, but cannot propagate. If the left side is greater than the right side, a propagating brittle fracture can occur at a shear stress equal to the yield stress. In effect, this equation describes a ductile-to-brittle transition.

The parameter  $k'$  determines the number of dislocations that are released from a pile-up at an obstacle to dislocation movement (such as a grain boundary) when a dislocation source is unlocked<sup>4</sup>. Materials with high values of  $k'$  (like iron and molybdenum) are prone to brittle fracture. Strengthening mechanisms that depend on dislocation locking usually cause embrittlement. The grain size should be interpreted as the slip-band length, or the distance that the first dislocation loop created by a Frank-Read source can move outwards before it is stopped by the grain boundary<sup>4</sup>. A fine grain size results in a short slip distance and a low transition temperature<sup>4</sup>. A coarse grain results in a long slip distance and a high transition temperature<sup>4</sup>.

A high value of frictional resistance ( $\tau_i$ ) promotes brittle fracture, since high stresses are required before yielding occurs. The highly directional bonding in ceramics, for instance, leads to a high  $\tau_i$  value and high inherent hardness and brittleness<sup>4</sup>. In body centered cubic (BCC) metals, the frictional resistance decreases rapidly with decreasing temperature and this leads to a ductile-to-brittle transition<sup>4</sup>. In equation (2.1),  $d^{1/2}$  enters as the product of  $\tau_i$ , so that a fine-grain material can withstand a higher value of  $\tau_i$  (or lower temperatures) before becoming brittle. The term  $\beta$  is related to the negative effects of a notch, and the  $\gamma_s$  term increases with the number of available slip systems and the size of the plastic region at the crack tip<sup>4</sup>. Plumtree and Gullberg applied equation (3.1) to ferritic stainless steels, and suggested the following modification<sup>1</sup>

$$\sigma_y k_y d^{1/2} = k_y^2 + \sigma_0 k_y d^{1/2} \geq C\mu\gamma \dots\dots\dots (3.2)$$

where  $\sigma_y$  = the flow stress or the fracture stress (coincident at the DBTT)

$k_y$  = the Hall-Petch slope

$d$  = the grain diameter

$\sigma_0$  = the lattice friction stress

$\gamma$  = the effective crack surface energy

C = a constant related to the stress state

Taking  $\sigma_0$  as the major temperature dependent term in equation (3.2), Petch derived a relationship between transition temperature and critical grain size of the form<sup>1</sup>:

$$DBTT = F + G \ln(d^{1/2}) \dots\dots\dots(3.3)$$

where F and G are constants.

Ductile-brittle-transition-temperature (DBTT) results obtained by Gooch and Ginn<sup>1</sup> for 12% chromium steels welded with an austenitic filler metal, represent a fair fit to the straight line suggested by equation (3.3), if the temperature for an absorbed impact energy of 30J from a standard Charpy specimen is plotted against  $\ln(d^{1/2})$ . These results (figure 3.4) clearly indicate that ferrite grain growth in the HAZ has a major influence on the impact properties of the welded joint.

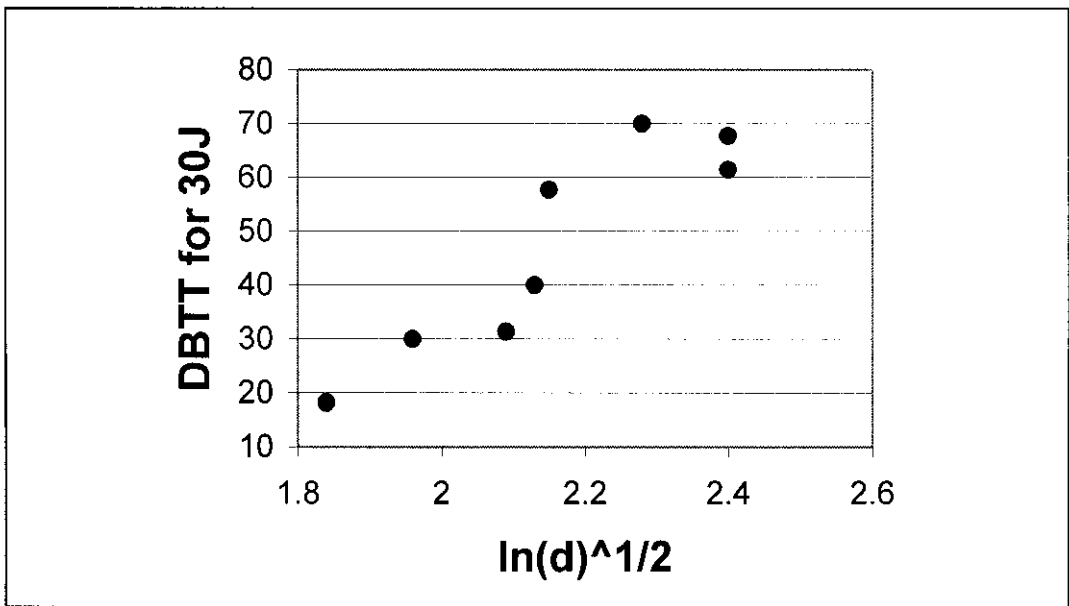


**Figure 3.4:** The effect of HAZ ferrite grain size on toughness of 12%Cr martensitic-ferritic steels<sup>1</sup>.

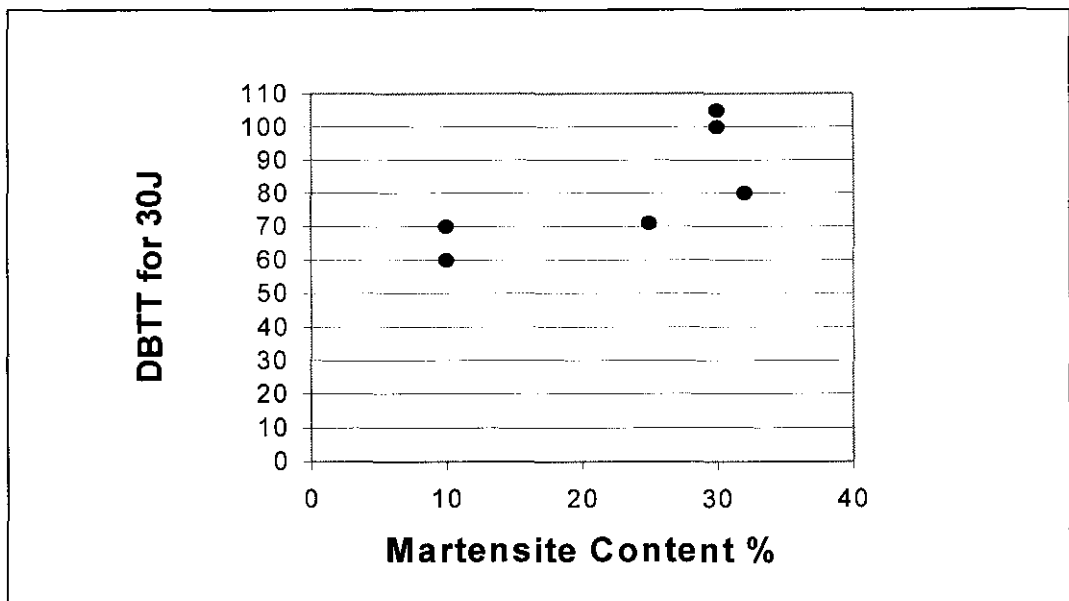


Figure 3.5: The effect of HAZ martensite on the toughness of 12% Cr martensitic-ferritic steels<sup>1</sup>.

The phase composition of the HTHAZ also influences the impact properties. The influence of martensite on toughness was studied by Gooch and Ginn<sup>1</sup>. Their results are shown in figure 3.5. The influence of martensite is not clear from the figure, but there is a trend for the DBTT's to increase at higher martensite contents. However, fractographic examination by Gooch and Ginn<sup>1</sup> indicated that some cleavage fractures originated at martensite colonies, and it seems that martensite in a predominantly ferritic structure facilitates cleavage initiation. Intergranular martensite would inhibit the transmission of slip from one grain to another, effectively raising the  $k_y$  term in equation (3.2) and acting as an internal stress raiser<sup>1</sup>. These effects would be more severe with increasing martensite hardness.

The comments made by Gooch and Ginn<sup>1</sup> assume that fracture occurs in a predominantly ferritic matrix. If the major phase is martensite, the situation would be different<sup>1,2,7,8</sup>. Metallographic examination by Gooch and Ginn<sup>1</sup> also showed subsidiary cleavage to be arrested at martensite colonies, and with increased martensite, this effect would increase the total amount of energy absorbed during fracture<sup>1</sup>. Furthermore, ferrite grain growth would be minimized by the increased

austenitic range at high temperatures. This suggests that improved toughness would be obtained at high martensite fractions<sup>1</sup>.

### 3.4 Summary

Although substantial  $\delta$ -ferrite grain growth occurs in the high temperature heat affected zone, brittle failure of welded joints in 3CR12 rarely happens during service. A number of explanations may be offered to account for this apparent contradiction.

In the first place, the fracture toughness is dependent on the plate thickness, and a weld in a thinner section may exhibit a lower DBTT than a weld in a thicker section. Furthermore, it appears as if the coarse grained zone is protected from brittle failure by plastic deformation of the relatively soft parent metal and weld metal. The alignment of the fusion line relative to the direction of the force is also of importance. If the heat-affected zone is not aligned properly with the notch (crack tip) during testing, the crack may simply propagate into another region of the weld.

Grain growth in the heat-affected zone (HAZ) does however cause concern. Work performed by Gooch and Ginn<sup>1</sup> clearly shows the detrimental influence of grain growth in the welded joint. Their comments are valid for a predominantly ferritic structure, and suggest that the presence of martensite colonies may have an adverse effect on the toughness of the heat-affected zone. Their results also show an increase in DBTT at higher martensite contents. However, they also found cleavage to be arrested by martensite colonies. In a predominantly martensitic structure this effect would be more significant, and the total energy absorbed by the joint during fracture may increase. If the high temperature heat affected zone can be prevented from entirely transforming to  $\delta$ -ferrite during welding, grain growth may be inhibited. The structure may also be predominantly martensitic after cooling, causing the impact energy of the heat affected zone to increase.

### 3.5 References

1. Gooch, T.G. & Ginn, B.J.; Heat affected zone toughness of MMA welded 12%Cr martensitic - ferritic steels; Report from the cooperative research programme for research members only; The welding institute; Cambridge;1988; pp. 3-9.
2. Zaayman, J.J.J.; The heat affected zone toughness of welds in 11 to 12 per cent chromium steels; M.Eng UP (1992); pp.31-71.
3. Hale, G.E.; Wide plate testing of welded 3CR12 martensitic/ferritic stainless steel; Report for Middelburg Steel an Alloys (Pty) Ltd; July 1990; pp. 1-9.
4. Dieter, G. E.; Mechanical Metallurgy; McGraw-Hill Book Company; London; SI Metric Edition 1988; pp. 483-487.
5. Reed-Hill, R.E. & Abbaschian, R; Physical Metallurgy Principles; PWS-KENT Publishing Company, Boston, Massachusetts; Third Edition 1992; pp. 795-796
6. Product Guide for 3CR12; Middelburg Steel and Alloys (Pty) Limited; January 1988; pp. 14-19
7. Grobler, C; Weldability Studies on 12% and 14% Chromium Steels; Ph.D. UP (1987); pp.14-62.
8. Pistorius, P.G.H.; The transformation kinetics of austenite to ferrite in dual phase 12% chromium steels; Ph.D UP (1992); pp. 12-40.

## CHAPTER 4

### The influence of interstitial carbon and nitrogen diffusion through the fusion line on the high temperature heat affected zone.

#### 4.1. Introduction

It was suggested earlier that grain growth in the high temperature heat affected zone might be suppressed by increasing the levels of carbon and nitrogen in this region. Diffusion from the weld metal into the heat-affected zone was proposed as a method of increasing the interstitial levels locally. This chapter discusses the experimental procedure followed to test the approach and the results obtained.

The iron-chromium system can give rise to a wide variety of microstructures with markedly different mechanical properties. A particular characteristic of the iron-chromium equilibrium diagram (figure 4.1) is the restricted austenite phase field in the Fe-rich part of the diagram, most often called the gamma loop ( $\gamma$ -loop).

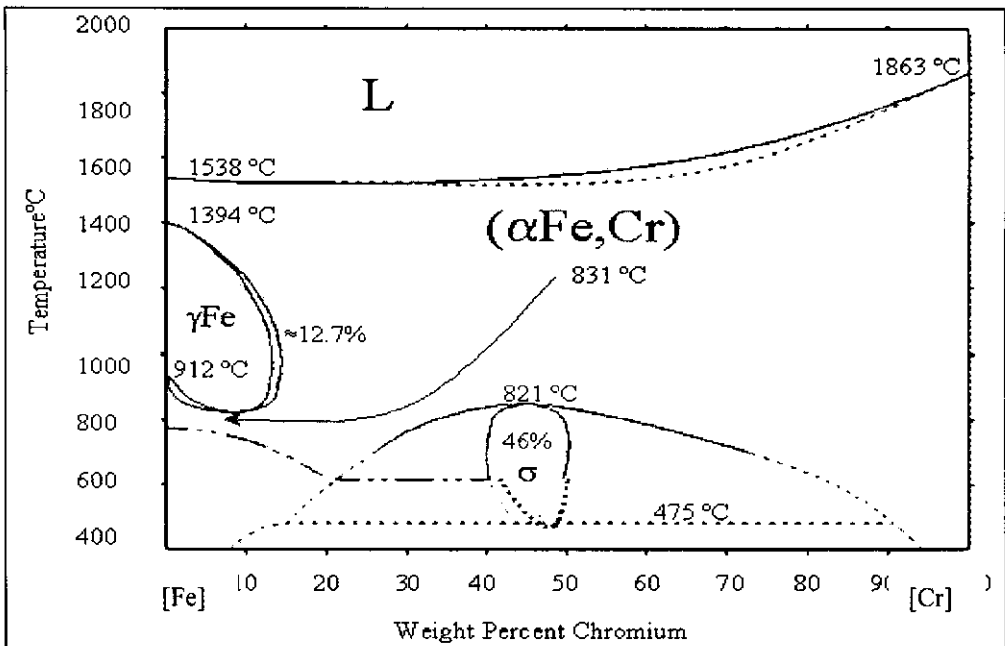


Figure 4.1: The iron-chromium equilibrium diagram.



The size of the gamma loop is essentially dependent on the relative amounts of austenite- and ferrite-formers in the steel. Elements like aluminum, vanadium, molybdenum, silicon and tungsten behave like chromium and promote the formation of delta ferrite<sup>1</sup>. Ferrite-formers tend to reduce the size of the gamma loop on the iron-chromium equilibrium diagram. On the other hand, elements like copper, manganese, cobalt, carbon and nitrogen behave like nickel and promote the formation of austenite<sup>1</sup>. Austenite-formers expand the gamma loop on the iron chromium diagram.

#### 4.1.1 The influence of martensite

The room temperature microstructure of chromium steels can be predicted in part by considering two effects, namely<sup>1</sup>

1. The balance between austenite- and ferrite-formers, which dictates the microstructure at elevated temperatures.
2. The overall alloy content, which controls the  $M_s$ - and  $M_f$ - temperatures and the fraction retained austenite at ambient temperature.

A convenient method of relating composition and microstructure in stainless steel welds is by means of the Schaeffler diagram. This diagram is illustrated in figure 4.2. The Ni-equivalent equation used in the diagram indicates that carbon and nitrogen are approximately thirty times more effective in forming austenite than nickel. Although the Schaeffler diagram is only approximately correct for slow cooling rates, the fairly rapid cooling that takes place in a weld and its vicinity makes the diagram a useful tool in predicting the phase balance of stainless steel weld metals.

The Schaeffler diagram only provides information regarding the phase composition of the weld metal. The chemical composition of the heat-affected zone generally does not change during welding, and the region only determines the microstructure and phase composition by the thermal cycle experienced.

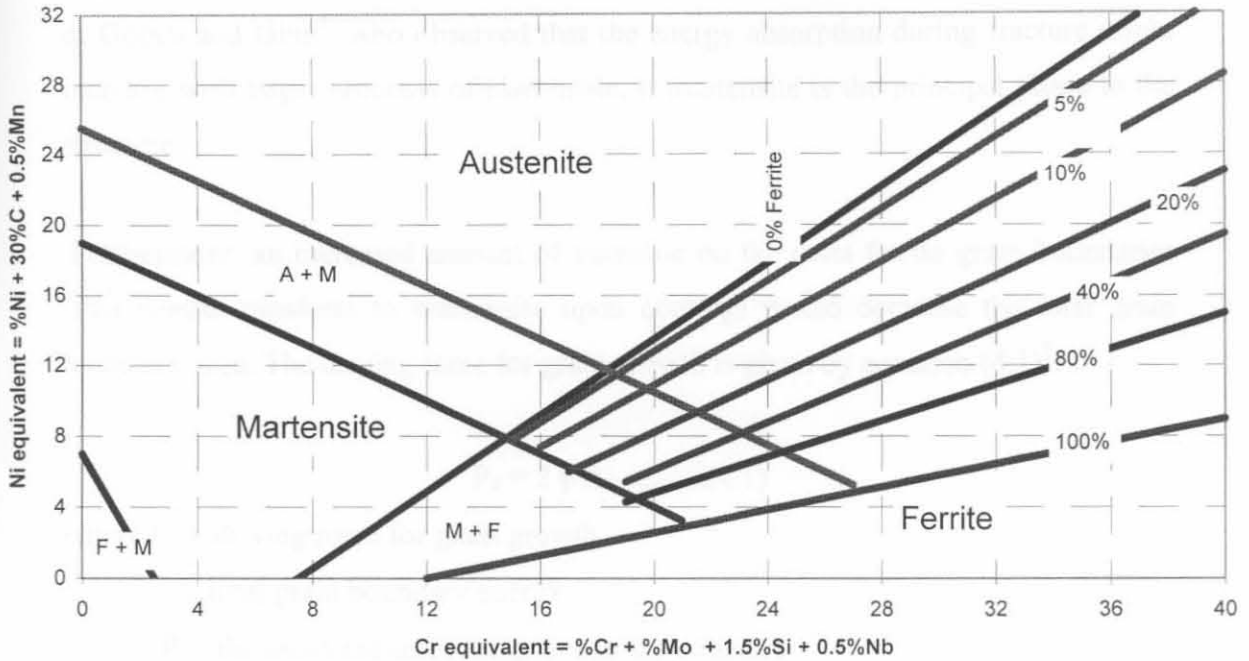


Figure 4.2: The Schaeffler diagram<sup>2</sup>.

Ferrite grain growth takes place in the high temperature heat affected zone at temperatures above the austenite to delta ferrite transformation temperature, and leads to embrittlement of the zone. This may play a role in increasing the transition temperature<sup>3,4,5</sup>.

Embrittlement may also occur in the weld metal, especially if a titanium or niobium stabilized filler metal is used<sup>6</sup>. The stabilizing precipitates decompose during welding, and re-precipitate in a finer form. Some of the titanium in the precipitate is replaced by chromium. As a result, residual titanium is present in the weld metal. The free titanium embrittles the weld metal, and has a negative effect on the impact properties of the joint<sup>6</sup>. However, this thesis is primarily concerned with embrittlement in the high temperature heat affected zone. In the heat-affected zone, ferrite grain growth is the major factor contributing to the embrittlement of the welded joint<sup>1,3,4,5</sup>.

In the HTHAZ of 3CR12 welds, significant amounts of martensite are often present on the grain boundaries. The presence of martensite also has an influence on the

impact properties of the joint. In the previous chapter reference was made to the work of Gooch and Ginn<sup>5</sup>, who observed that the energy absorption during fracture might increase with larger amounts of martensite, if martensite is the principal phase in the structure.

Furthermore, an increased amount of austenite on the delta ferrite grain boundaries (that would transform to martensite upon cooling) would decrease the total grain boundary area. The driving force for grain growth is given by equation (4.1)<sup>7</sup>:

$$P_d = 2 \gamma/R \dots\dots\dots(4.1)$$

where  $P_d$  = driving force for grain growth

$\gamma$  = total grain boundary energy

$R$  = the mean radius of the grains in the structure

The  $\gamma$  -term, or the total grain boundary energy of the delta ferrite grains, would be reduced by the presence of a second phase (in this instance austenite) on the grain boundaries<sup>7</sup>. A second phase on the grain boundaries also acts as a physical obstacle to grain boundary movement, and the grain boundary must physically pull itself through the second phase inclusions in order for grain growth to take place<sup>8</sup>.

The influence of large fractions of martensite in the heat-affected zone was studied during weld simulation experiments carried out by Zaayman<sup>3</sup>. The results were obtained by applying different thermal cycles to the same alloy. From the results (as shown in figure 4.3) it appears that increasing martensite levels are harmful to the impact properties of the structure up to a fraction of 90%, and that the DBTT decreases thereafter. The martensite on the grain boundaries induces high stresses in the softer adjacent ferrite. These stresses promote cleavage fracture<sup>3</sup>. An increase in the fraction martensite also decreases the effective grain size of the remaining ferrite. At higher fractions of martensite this effect dominates, and this accounts for the observed decrease in the DBTT<sup>3</sup>.

#### 4.1.2 The influence of carbon and nitrogen.

Carbon and nitrogen influence the impact properties of the heat-affected zone mainly in two opposing ways. In the first instance, the hardness of the intergranular martensite that forms in the high temperature heat affected zone increases with increasing carbon and/or nitrogen contents, which is detrimental to the impact properties<sup>3</sup>. Carbon and nitrogen are also strong austenite-formers, and can restrict delta ferrite grain growth by extending the dual phase austenite-ferrite structure to high temperatures<sup>3</sup>. The optimum amount of carbon and nitrogen is strongly dependent on the alloy content of the steel, and may therefore vary considerably. The combined effect of carbon and nitrogen on the size of the  $\gamma$ -loop is shown in figure 4.4. Although the microstructure of the heat affected zone in as-welded 3CR12 is not predominantly martensitic, an increase in the interstitial carbon and nitrogen contents of the heat affected zone could shift the  $\%(C+N)$  closer to the optimum indicated in figure 4.5.

In the case of a predominantly ferritic microstructure with a large ferrite grain size and grain boundary martensite, a higher carbon and nitrogen content may be detrimental to the impact properties of the joint. The martensite on the grain boundaries would be harder and more brittle with a higher interstitial content. If the structure contains a high fraction of martensite, the effect on the impact properties of the joint would be undesirable.

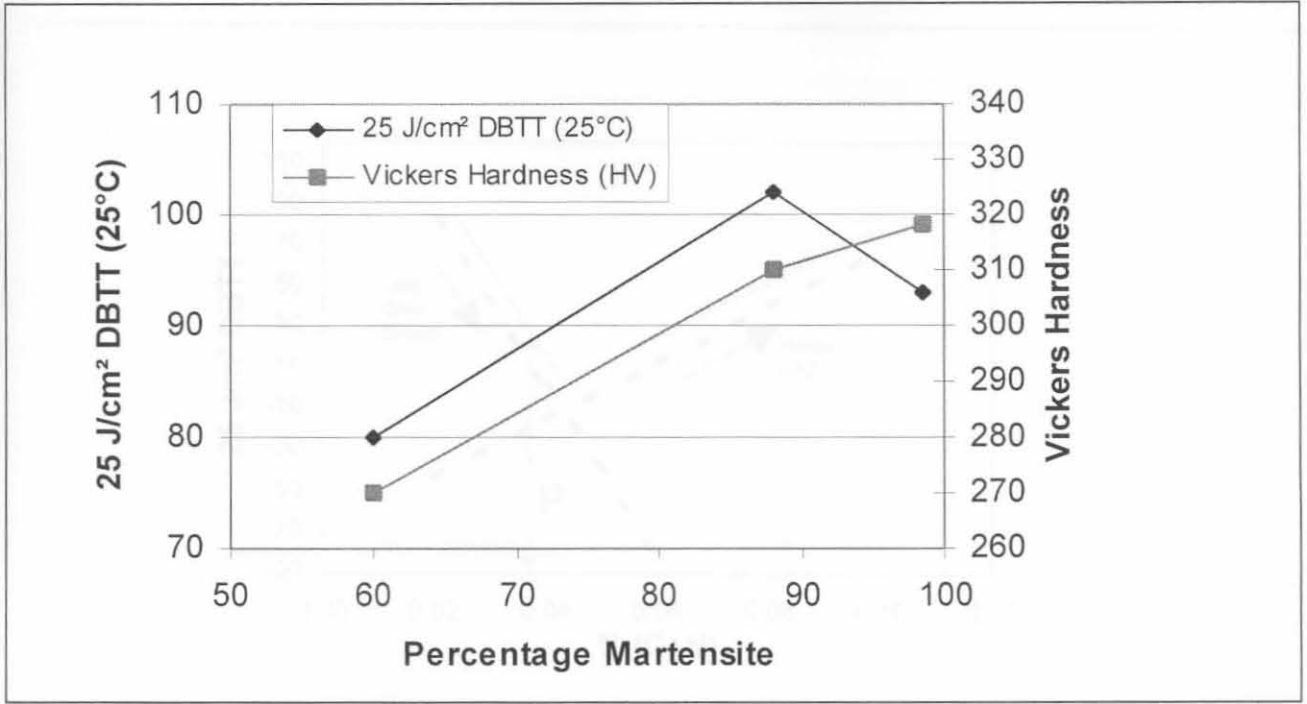


Figure 4.3: The influence of martensite content on the DBTT at a constant ferrite grain size<sup>3</sup>.

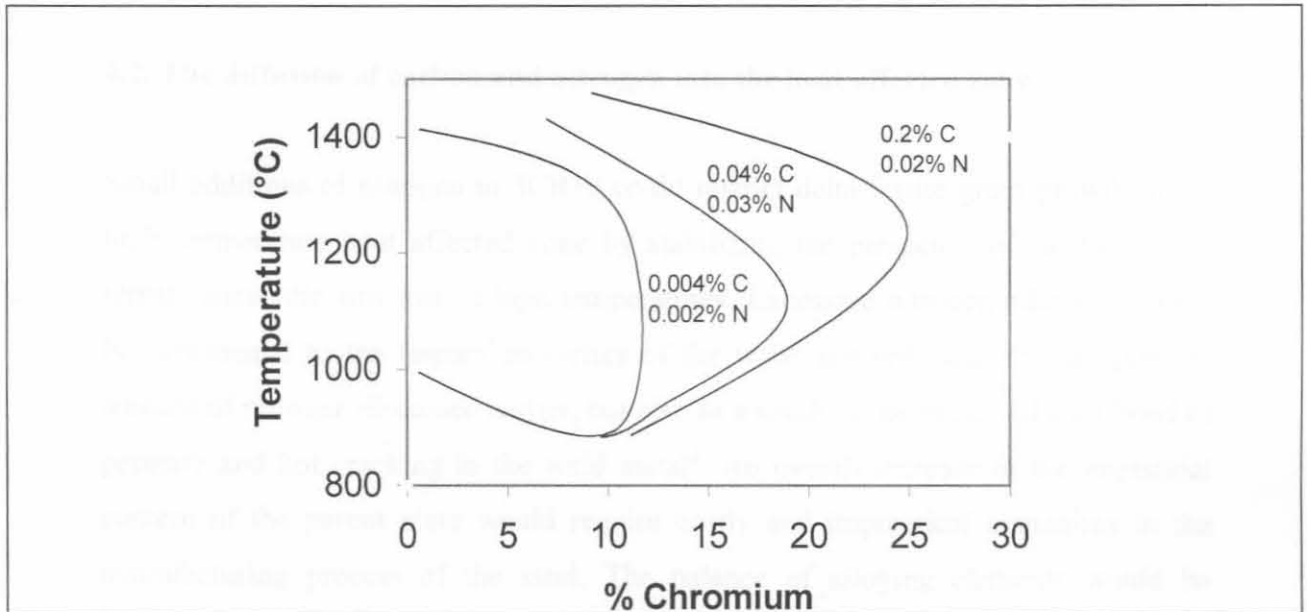


Figure 4.4: The influence of carbon and nitrogen on the size of the gamma loop on the Fe-Cr system<sup>3</sup>.

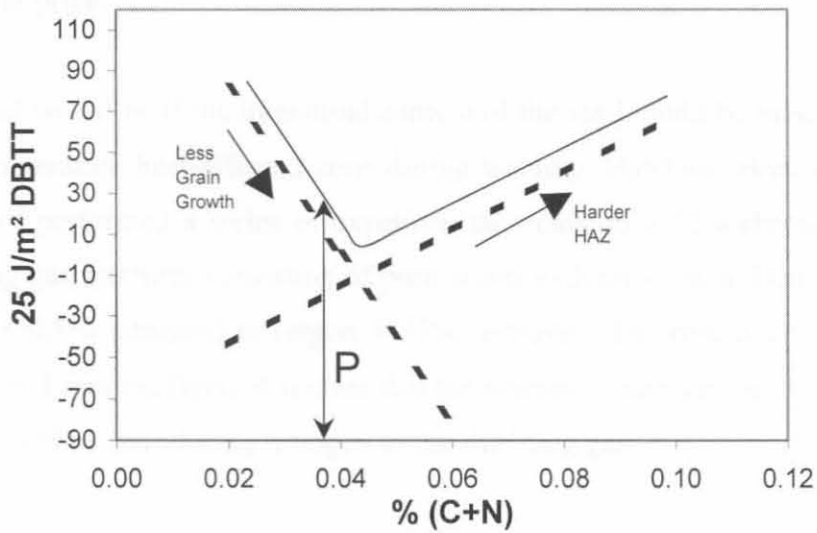


Figure 4.5: The influence of carbon and nitrogen on the DBTT of a predominantly martensitic structure<sup>3</sup>.

#### 4.2. The diffusion of carbon and nitrogen into the heat affected zone

Small additions of nitrogen to 3CR12 could restrict delta ferrite grain growth in the high temperature heat affected zone by stabilizing the presence of a dual phase ferritic-austenitic structure at high temperatures. Excessive nitrogen additions would be detrimental to the impact properties of the weld, not only due to the optimum amount of nitrogen discussed earlier, but also as a result of the increased likelihood of porosity and hot cracking in the weld metal<sup>2</sup>. An overall increase in the interstitial content of the parent plate would require costly and impractical alterations in the manufacturing process of the steel. The balance of alloying elements would be disturbed and various heat treatment steps in the process would have to be altered. As one of the main advantages of 3CR12 is the relatively economical cost at which the steel can be made available to the consumer, an increase in the overall interstitial content, with subsequent alterations in the manufacturing process would not be practical. Increased carbon levels would necessitate an increase in chromium levels in



order to prevent sensitizing, which would inflate the raw material cost and the consumer price.

The ideal would be if the interstitial content of the steel could be raised locally in the high temperature heat-affected zone during welding. Hawkins, Beech and Valtierra-Gallardo<sup>9</sup> performed a series of experimental welds on a 12% chromium steel with shielding gas mixtures consisting of pure argon with nitrogen additions ranging from (argon + 0.5% nitrogen) to (argon + 75% nitrogen). The results are summarized in figure 4.6. From the figure it is clear that the amount of nitrogen in the weld metal can be increased by introducing nitrogen to the shielding gas.

In order to change the nitrogen content in the HTHAZ, nitrogen has to diffuse from the weld metal into the HAZ adjacent to the weld. If the fusion line is seen as a simple diffusion couple at a constant temperature, the concentration profile of nitrogen away from the fusion line into the parent metal can be represented by figure 4.7.

The concentration of nitrogen at a specific distance from the fusion line as represented by figure 4.7, is described by equation (4.2)<sup>10</sup>, if interstitial diffusion into the heat affected zone is assumed to be equivalent to interstitial case hardening by diffusion, and geometrical effects are not taken into account. The geometrical shape of particles in a particle bed influences reaction rates to a great extent, but the geometrical effect can be neglected when the process is assumed to be similar to the case hardening of steel components in carbon or nitrogen rich atmospheres.

$$c = c_0 \operatorname{erfc} \left\{ \frac{r}{2(Dt)^{1/2}} \right\} \dots\dots\dots(4.2)$$

where  $c_0$  = nominal concentration of nitrogen in the weld metal (the relative solubilities in the liquid and the solid austenite should in reality be used)

$c$  = concentration of nitrogen at a distance  $r$  from the fusion line

$r$  = distance from the fusion line (cm)

$D$  = diffusion coefficient for nitrogen in steel at the temperature at which diffusion takes place

$t$  = time in seconds

$(Dt)^{1/2}$  = the diffusion distance as defined by Einstein (from Thelning<sup>10</sup>)

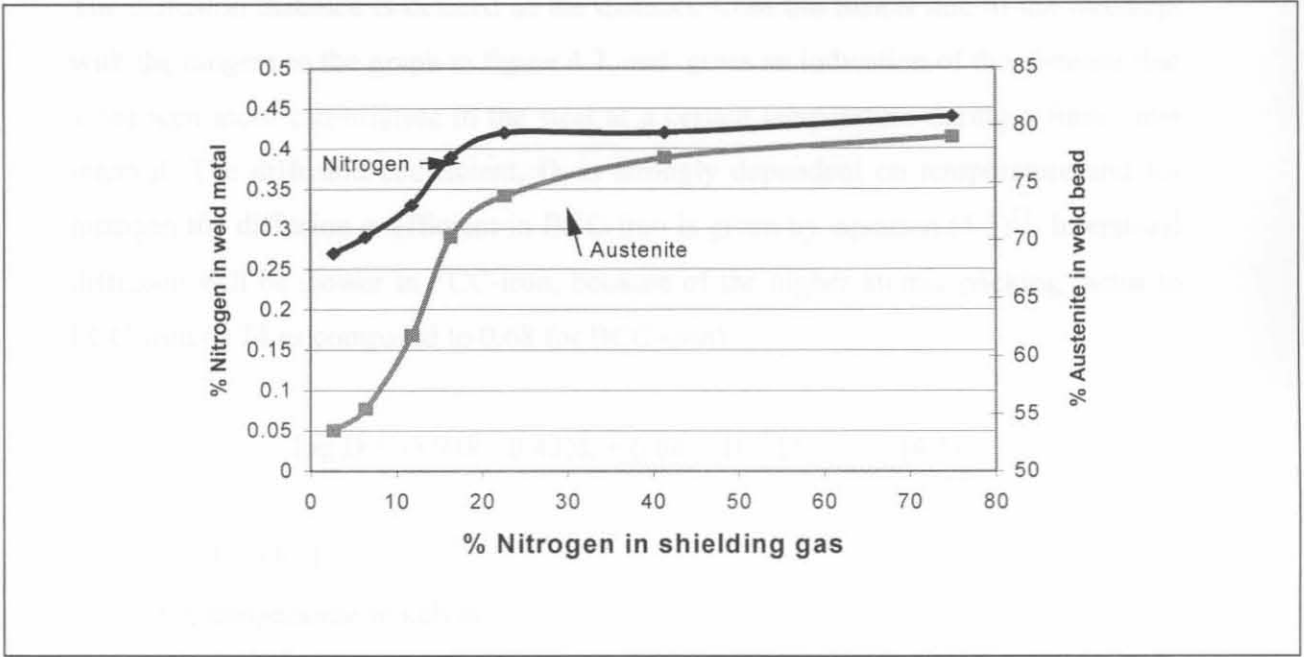


Figure 4.6: The nitrogen content of the weld metal as a function of the nitrogen content of the shielding gas during GMAW welding<sup>9</sup>.

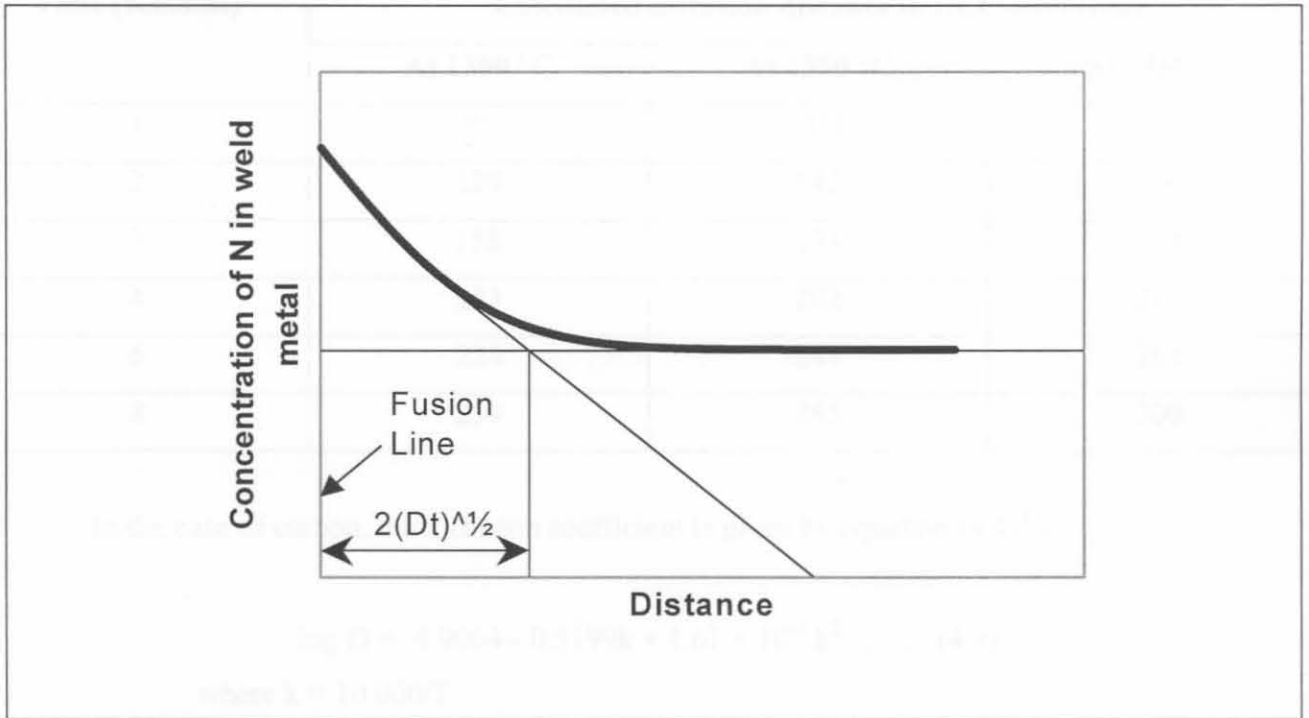


Figure 4.7: The concentration of nitrogen away from the fusion line into the parent metal after diffusion for time  $t$  at a constant temperature.



The diffusion distance is defined as the distance from the fusion line to the intercept with the tangent to the graph in figure 4.7, and gives an indication of the distance that a nitrogen atom can migrate in the steel at a certain temperature during a finite time interval. The diffusion coefficient,  $D$ , is strongly dependent on temperature and for nitrogen the diffusion coefficient in BCC-iron is given by equation (4.3)<sup>11</sup>. Interstitial diffusion will be slower in FCC-iron, because of the higher atomic packing factor in FCC-iron (0.74 as compared to 0.68 for BCC-iron)

$$\log D = -5.948 - 0.433k + 6.08 \times 10^{-4} k^2 \dots\dots\dots(4.3)$$

where  $k = 10\,000/T$

$T$  = temperature in kelvin

Using equations (4.2) and (4.3) the calculated diffusion distance was calculated for nitrogen at 1300 °C, 1350 °C and 1380 °C for intervals from 1s to 8s. The results are shown in table 4.1.

Table 4.1: Diffusion distances for nitrogen in BCC-iron at different temperatures.

Time (seconds)	Calculated diffusion distance in BCC-iron (µm)		
	At 1300 °C	At 1350 °C	At 1380 °C
1	91	100	106
2	129	142	150
3	158	174	184
4	183	202	213
6	224	247	261
8	259	285	300

In the case of carbon, the diffusion coefficient is given by equation (4.4)<sup>11</sup>.

$$\log D = -4.9064 - 0.5199k + 1.61 \times 10^{-3} k^2 \dots\dots\dots(4.4)$$

where  $k = 10\,000/T$

$T$  = temperature in kelvin

The diffusion distance for carbon in BCC-iron was calculated in the same way as for nitrogen, and the results are shown in table 4.2.

Table 4.2: Diffusion distances for carbon in BCC-iron at different temperatures.

Time (seconds)	Calculated diffusion distance in BCC-iron ( $\mu\text{m}$ )		
	At 1300 °C	At 1350 °C	At 1380 °C
1	169	189	202
2	238	267	286
3	293	328	350
4	338	378	404
6	414	463	495
8	478	535	571

Isothermal conditions are implicitly assumed in the above calculations. This assumption is not valid, as the welded plate is cooling continuously. The temperature cycle experienced by a point at any distance away from the center line of a weld can be predicted using the Rosenthal equation. The Rosenthal equation assumes heat flow from a point source, which implies that the temperature at this point (at the weld centre line) reaches infinity. The equation also assumes that the material properties (thermal capacity, diffusivity, conductivity) do not change with temperature and it neglects heat losses at the plate surface, as well as the latent heat change due to any phase transformations that may occur. In spite of these limitations, the temperature field in the heat-affected zone is well represented by the Rosenthal equation<sup>2</sup>. In most practical welding situations, the velocity of the arc along the workpiece is much higher than the thermal diffusion rate. In other words, heat flow in the direction of travel is small compared to that perpendicular to the travel direction<sup>2</sup>. Furthermore, for a given weld geometry, material and process, the cooling time through the range 800 °C to 500 °C is constant in the heat affected parent plate.

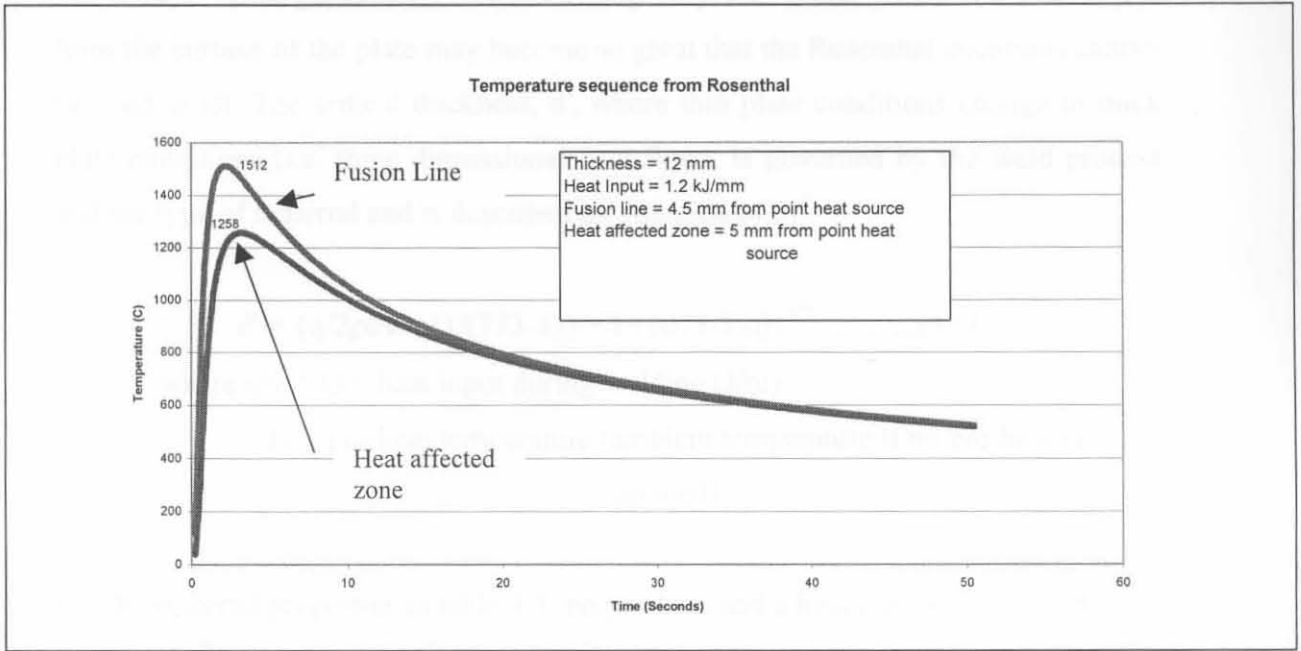


Figure 4.8: The welding temperature sequence as predicted from the Rosenthal equation<sup>2</sup>.

On the basis of these assumptions, Rosenthal<sup>2</sup> determined the solutions to the heat flow equations of a moving point heat source in 1935<sup>2</sup>. Good evidence exists that the Rosenthal equations have agreeable validity in describing the temperature distribution about a weld<sup>2</sup>. In order to solve the equation, certain thermal and material properties of the parent plate are required in the Rosenthal equation. Various sources<sup>2,12,13,14</sup> were used to obtain these properties for the 3CR12 parent plate. The properties are tabulated in table 4.3.

Table 4.3: Thermal and material properties for 3CR12.

Melting Point	Specific Gravity ( $\rho$ )	Specific Heat (C)	Thermal Conductivity ( $\lambda$ )	$\rho C$
1773 K	7700 kg/m <sup>3</sup>	510 J/kgK	26 J/msK	$3.93 \times 10^6$ J/m <sup>3</sup> K

Rosenthal derived two different equations for thick and thin plate conditions. In the thin plate equation heat flow is considered to be two-dimensional. This assumption is

not always valid, particularly when welding very thin plate, where the heat losses from the surface of the plate may become so great that the Rosenthal equations cannot be used at all. The critical thickness,  $d'$ , where thin plate conditions change to thick plate conditions (i.e. three dimensional heat flow), is governed by the weld process and the type of material and is described by equation (4.5)<sup>2</sup>.

$$d' = \{q/2\rho cv \times [1/(773-T_0) + 1/(1073-T_0)]\}^{1/2} \dots\dots\dots(4.5)$$

where  $q/v = Q =$  heat input during welding (J/m)

$T_0 =$  pre-heat temperature (ambient temperature if no pre-heat is applied)

For the material properties in table 4.3, no pre-heat and a heat input during welding of  $Q = 1 \times 10^6$  J/m,  $d'$  equals 21mm. Therefore, the thin plate equation must be used to predict the temperature cycle in a 12 mm 3CR12 plate. The Rosenthal equations for thin plate conditions are given by equations (4.6) through (4.9).

$$T_p - T_0 = (2/\pi e)^{1/2} \times Q/(d\rho c 2r) \dots\dots\dots(4.6)$$

$$\Delta t = Q^2/(4\pi\lambda\rho c\Theta_2^2 d^2) \dots\dots\dots(4.7)$$

$$1/\Theta_2^2 = 1/(773-T_0)^2 - 1/(1073-T_0)^2 \dots\dots\dots(4.8)$$

$$T - T_0 = \Theta_2 \times (\Delta t/t)^{1/2} \times \exp \{-[\Theta_2^2 \Delta t]/[2et(T_p - T_0)^2]\} \dots\dots\dots(4.9)$$

where  $d =$  plate thickness

$r =$  distance from the point-heat source perpendicular to the welding direction

$e =$  the base of natural logarithms ( $e \approx 2.718$ )

$T_p =$  peak temperature reached at distance  $r$

The other variables are defined in table 4.3.

Assuming that the fusion line represents a peak temperature equal to the liquidus temperature of 3CR12, calculation yields the distance from the point source to the fusion line ( $T_p = 1773K$ ) of a 1.0 kJ/mm weld on a 12mm 3CR12 plate to be 3.6mm.

The mean distance from the fusion line to the end of the grain growth zone is 200 $\mu$ m (ten measurements, 0.95 confidence level = 1.7 $\mu$ m). As a result, the end of the grain growth zone would be 3.8mm from the point source. If another 200 $\mu$ m is added for the remainder of the heat affected zone, the edge of the heat affected zone would be approximately 4mm from the point source. The measured value of 4.5mm from the center to the fusion line used in figure 4.8 was determined from a heat input of 1.2 kJ/mm, while welds used for this calculations were made at 1.0 kJ/mm. Through substitution and calculation, equation (4.9) can be written as

$$T-T_0 = 2328/t^{1/2} \times \exp [-(0.46/t)] \dots\dots\dots(4.10)$$

for the fusion line (3.6mm from the point source)

$$T-T_0 = 2328/t^{1/2} \times \exp [-(0.55/t)] \dots\dots\dots(4.11)$$

for the edge of the HTHAZ (3.8mm from the point source)

$$T-T_0 = 2328/t^{1/2} \times \exp [-(0.60/t)] \dots\dots\dots(4.12)$$

for the edge of the HAZ (4.0 mm from the point source)

The temperature cycles during the welding of 3CR12 plate can be calculated using equations (4.10) to (4.12). The area between fusion line and the edge of the coarse grain heat affected zone can be viewed as a series of successive peak temperatures to which the coarse delta ferrite structure is heated during welding.

It has already been stated that the nitrogen content of the weld metal can be increased effectively by adding nitrogen gas to a pure argon shielding gas<sup>7</sup>. The carbon content of the weld metal may be increased by welding with a filler metal containing a higher carbon content, such as E307.

The Rosenthal prediction (as shown in figure 4.8) states that the fusion line of a weld produced with a heat input of 1.2 kJ/mm in a 12 mm plate would be above 1400 °C for approximately 3 seconds. At a temperature of 1380 °C carbon can diffuse 202 $\mu$ m in 1 second and nitrogen can diffuse 106 $\mu$ m in the same time interval (see tables 4.1 and 4.2). This indicates that nitrogen can diffuse at least 106 $\mu$ m and carbon 202 $\mu$ m

away from the fusion line if the temperature were 1380°C or higher for 1 second in a weld performed with the same welding parameters.

The predicted diffusion data implies that it is possible to increase the interstitial content of the high temperature heat affected zone during welding by diffusion from the weld metal, as the measured width of the high temperature zone is in the proximity of 200µm. The width of the grain growth zone is typically a function of the heat input, but for the welding parameters used for the Rosenthal prediction, diffusion appears to be a practical method of increasing the interstitial content locally in the high temperature heat affected zone.

An increase in the interstitial content of the heat-affected zone would cause the gamma loop on the iron-chromium equilibrium diagram to expand. This will guarantee the existence of a larger amount of austenite on the delta ferrite grain boundaries at elevated temperatures during welding. The resulting decrease in total grain boundary energy would reduce the driving force for grain growth<sup>7</sup>, and would inhibit the delta ferrite grain growth that occurs in the high temperature heat affected zone.

### **4.3 Experimental welds and results**

In order to evaluate the effectiveness of the above-mentioned approach, a series of welds were produced using pure argon and argon-nitrogen shielding gas mixtures, or a high carbon filler metal. The microstructure and the toughness of the resulting welds were investigated.

#### **4.3.1 Gas metal arc welding with E309L**

The first series of welds were produced as a reference using the gas-metal-arc-welding process (GMAW) on a 12mm 3CR12 plate. Pure argon shielding gas and a 1.2mm diameter 309L filler wire were used. The heat input was maintained at 1.2 kJ/mm and a K-type weld preparation was utilized. The microstructures obtained in



the high temperature heat affected zone of the welds are typical of the microstructures discussed in the previous chapter, consisting of large delta ferrite grains with blocky martensite on the grain boundaries. A typical microstructure is shown in figure 4.9

The grain size in the high temperature heat affected zone was measured using two different methods. In the first place, a line intercept method was used. Four different counts of grain boundaries intercepting a line of constant length were made. Equation (4.13) (Hillards-equation) was used to determine the ASTM grain size number in the heat affected zone.

$$N = -10.0 - 6.64 \log [L/(nM)] \dots\dots\dots(4.13)$$

where L = length of line (cm)

n = amount of grain boundaries intercepting the line (the grain size was taken as the size of the ferrite + the martensite)

M = magnification

N = ASTM grain size number

Standard ASTM eyepieces were also used to determine the range of the grain size. The corresponding grain size in microns was also obtained from data in the ASTM standards, part 1-A, 1946. In the ASTM method,  $n = 2^{N-1}$ , where n equals the number of grains per square inch at a magnification of 100x. Consequently, the greater the value of N, the smaller the average diameter of the grains.

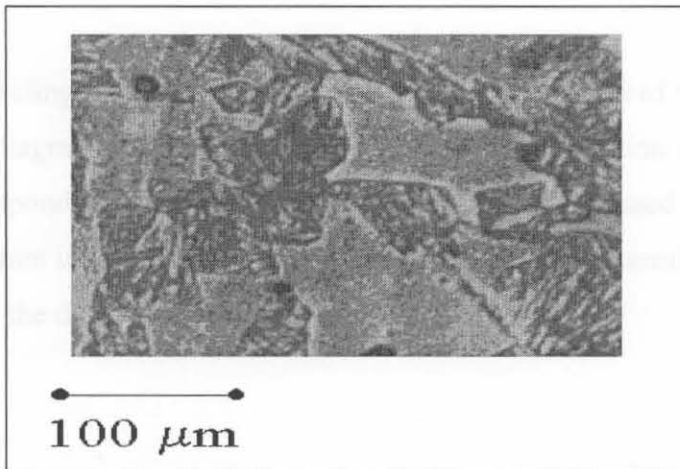


**Figure 4.9:** The high temperature heat affected zone. (GMAW, HI = 1.2 kJ/mm, 309L filler wire pure Argon shielding gas).

The ferrite number (which represents the magnetic response of the sample) of the weld metal was measured using a Fischer Feritscope™. The relationship between the ferrite number and the percentage ferrite is shown in figure 4.10. Ferrite number measurements are inherently more accurate than point counting. For this reason, the Feritscope was used to quantify the amount of ferrite in the weld metal. The average ferrite number obtained from ten different readings on each sample was 15.1FN. Using Kalling’s no. 2 to etch the samples, the ferrite is observed as a light coloured phase. Using figure 4.10, a ferrite percentage corresponding to a ferrite number of 15.1 could be determined. The weld metal was found to contain approximately 13.4% ferrite.

**Table 4.4:** ASTM grain size numbers in the high temperature heat affected zone (GMAW, 1.3kJ/mm, E309L filler wire, pure argon shielding gas)

Number	L (cm)	n	M	N	N from ASTM eyepiece	Matching grain size (µm)
1	25.1	5	400	2.6	1-2	200-300
2	25.1	5	400	2.6	1-2	200-300
3	25.1	4	400	1.9	1-2	200-300
4	25.1	4	400	1.9	1-2	200-300
Average				2.25		

A tie line connecting the parent metal position and the position of the filler metal on the Schaeffler diagram was used to estimate the amount of dilution in the weld metal. The line corresponding to the parent metal and filler metal used is shown on the Schaeffler diagram in figure 4.11. If 13.4% ferrite is used to determine the position of the weld metal, the dilution is estimated at 45%.



### 4.3.2 Charpy V-notch values at 20 °C

Fifteen Charpy specimens were machined from the welded plate. As mentioned earlier, a K-type weld preparation with a pre-welded layer on the flat side was used (see figure 3.3). Precise placement of the Charpy notch into the high temperature heat affected zone was still difficult, and weld metal, parent metal and heat affected zone failures occurred. The heat affected zone failures appeared bright and uneven. The parent metal fractures were ductile with considerable plastic deformation around the edges of the specimen. The weld metal failures were dull fractures with no or very little plastic deformation. The results of the impact tests are shown in figure 4.12. All the fractures obtained could be divided into either the HAZ, parent metal or weld metal failures, and it appears that if a crack initiated in the coarse grained heat affected zone, it would travel straight through the zone without swerving into the parent metal or the weld metal, and this resulted in very low impact energies being recorded for the heat affected zone failures. The conclusion can be drawn that the butter layer method is effective if the notch can be directed accurately into the heat affected zone, and that the true impact properties of the heat affected zone can be measured. The results also indicate that the impact properties of the heat affected zone are inferior to those of the weld and parent metal, but it has to be emphasized once again that the butter layer K-type preparation can be described as a worst case situation, and that intergranular heat affected zone failures rarely occur in practice<sup>1</sup>. It is important to realize that stress raisers in the coarse grained region should be avoided in practice, and that brittle fracture may occur if proper design and preparation procedures are not followed.

### 4.3.3 Shielded metal arc welding with E309L and E307

A high carbon austenitic shielded metal arc welding electrode is also commercially available in the market, and the use of these electrodes was investigated. The second series of welds were produced using shielded metal arc welding and 8mm 3CR12 plate. The heat input was maintained at 0.7kJ/mm. In order to investigate the influence of a higher carbon filler on the HTHAZ properties, two electrode were used,

containing 0.03% (E309L) carbon and 0.16% carbon (E307) respectively. The microstructure in the high temperature heat affected zone of the E307 weld, as shown in figure 4.13 contains higher fractions of martensite on the grain boundaries, while the grain size of the remaining ferrite is smaller than in the E309L weld. The microstructures in the weld metal of both welds consisted of austenite and ferrite, and the ferrite numbers obtained from Fischer Ferritscope readings were 15.5FN for the E309L electrode and 13.1FN for the E307 electrode respectively.

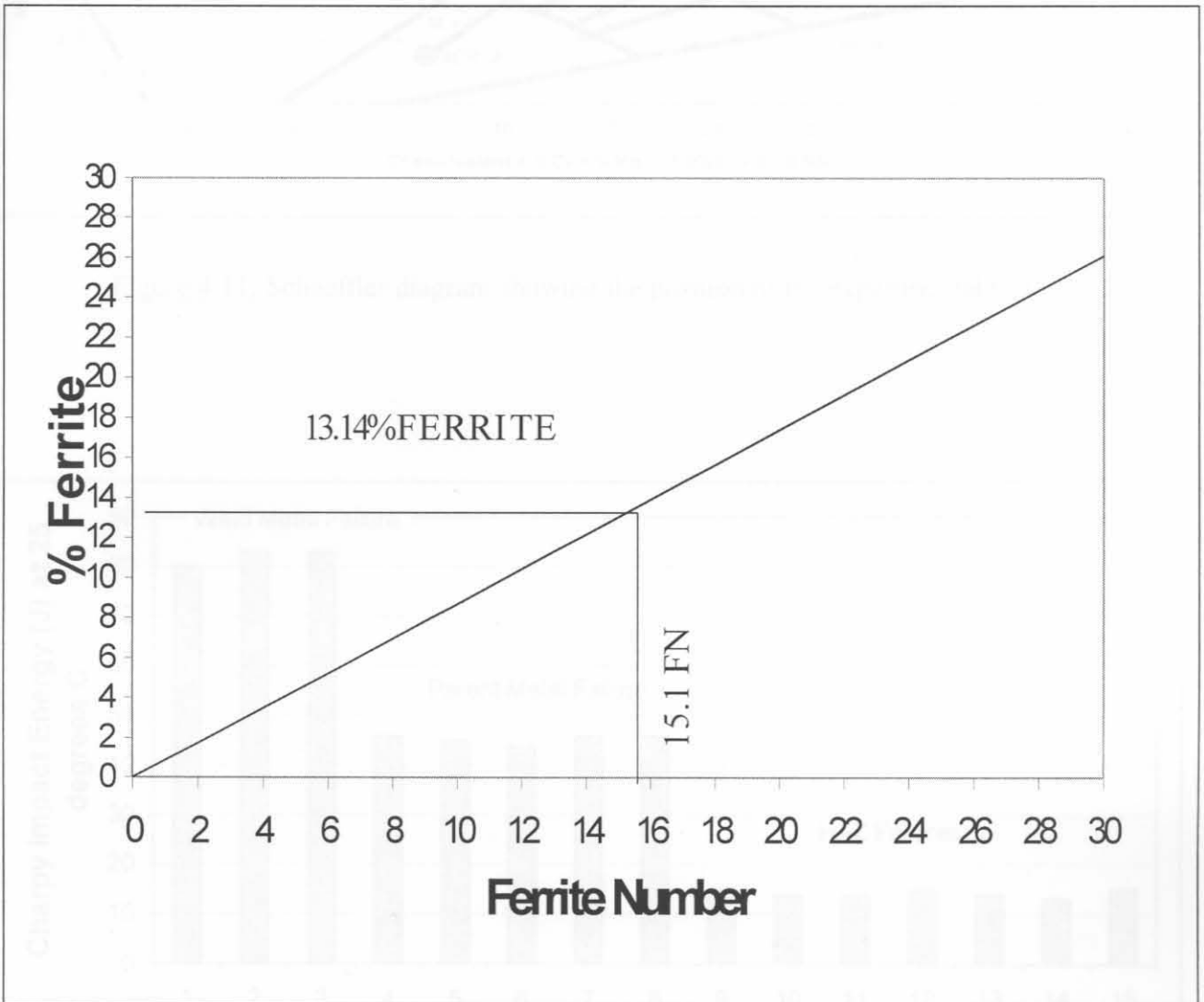


Figure 4.10: The relationship between ferrite number and percentage ferrite. (After the DeLong diagram, by William T. DeLong, revised January 1973)

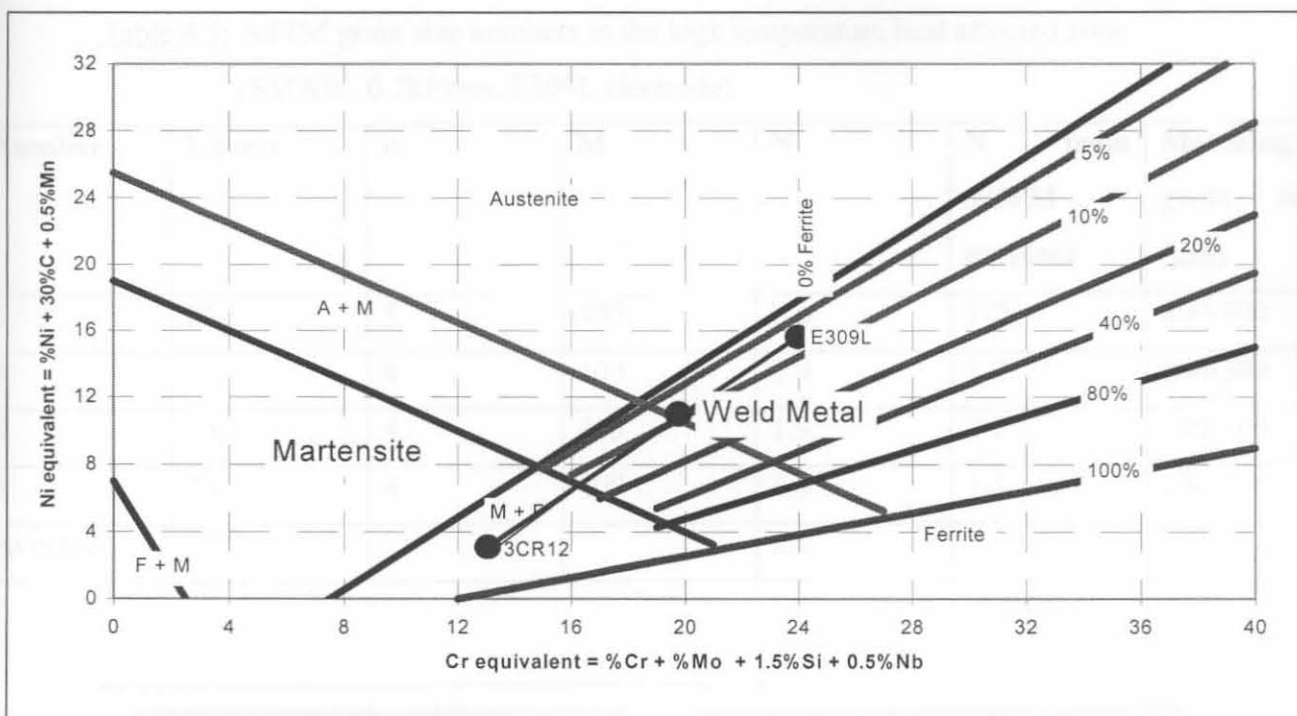


Figure 4.11: Schaeffler diagram showing the position of the experimental weld

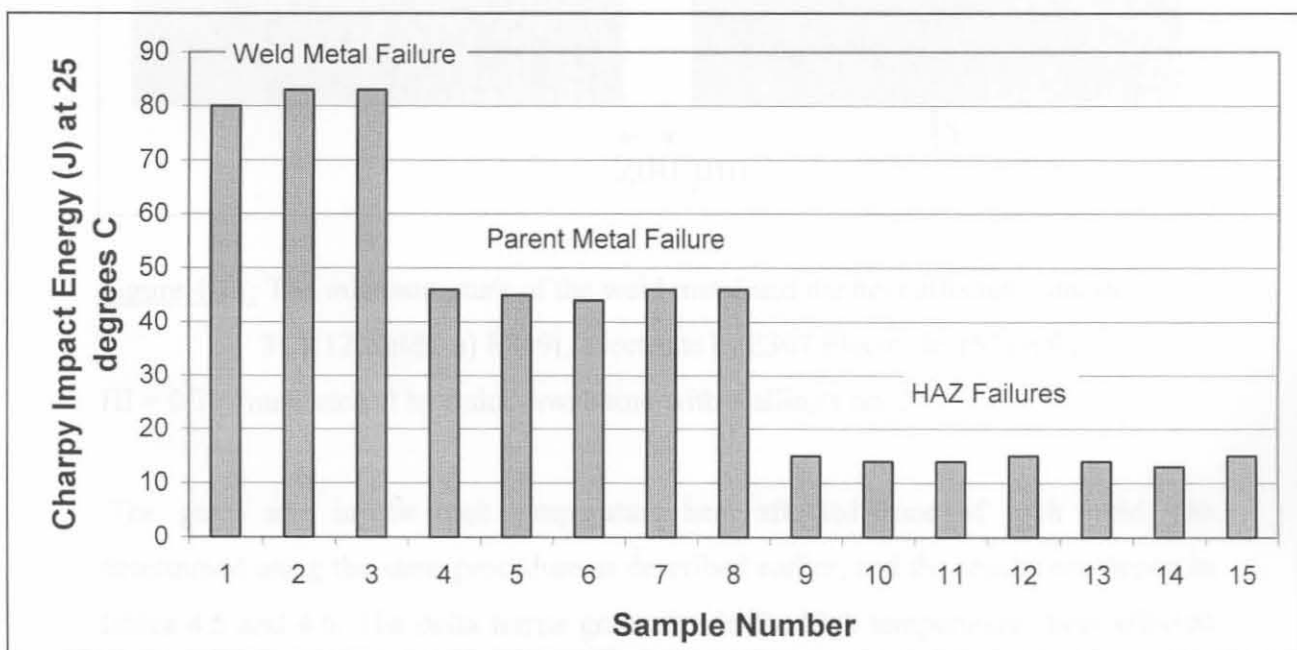
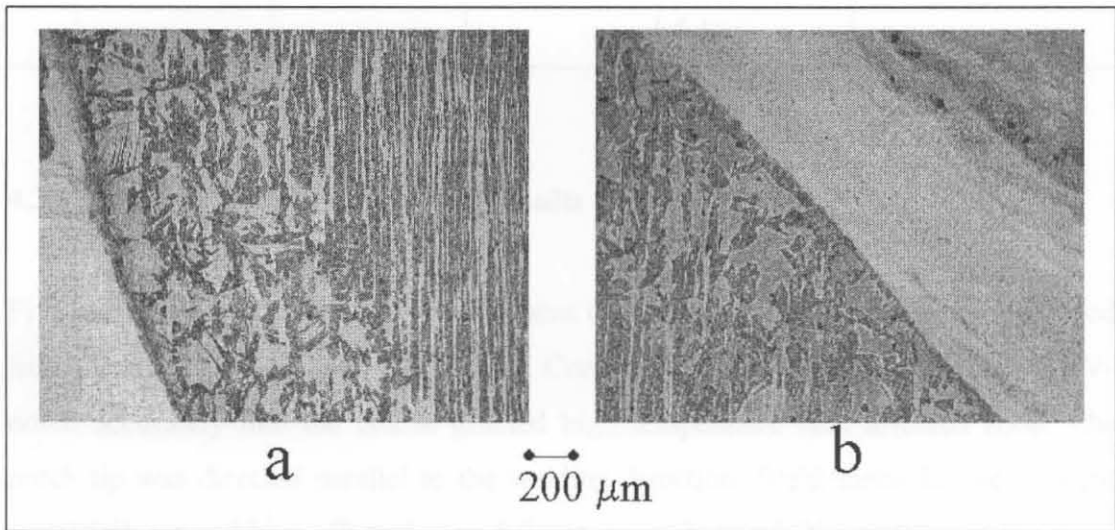


Figure 4.12: Charpy Impact Energy values at 25°C (GMAW, HI = 1.3kJ/mm, E309L filler wire, pure argon shielding gas)

**Table 4.5:** ASTM grain size numbers in the high temperature heat affected zone  
 (SMAW, 0.7kJ/mm, E309L electrode)

Number	L (cm)	n	M	N	N from ASTM eyepiece	Matching grain size (µm)
1	25.1	5	400	2.6	1-2	200-300
2	25.1	4	400	1.9	1-2	200-300
3	25.1	4	400	1.9	1-2	200-300
4	25.1	4	400	1.9	1-2	200-300
Average				2.1		



**Figure 4.13:** The microstructure of the weld metal and the heat affected zone in 3CR12 welds. a) E309L Electrode b) E307 Electrode. (SMAW, HI = 0.7kJ/mm, etched by quick swabbing with Kalling's no. 2)

The grain size in the high temperature heat affected zone of each weld was determined using the same procedure as described earlier, and the results are shown in tables 4.5 and 4.6. The delta ferrite grain size in the high temperature heat affected zone of E307 welds is smaller than the grain size obtained in the coarse grained zone of E309L welds. Furthermore, a larger fraction of martensite is present on the ferrite grain boundaries of E307 welds. Image analysis readings yielded 43% martensite on the delta ferrite grain boundaries in the high temperature heat affected zone of the



E307 welds, and 34% grain boundary martensite in the corresponding zone of the E309L welds.

**Table 4.6:** ASTM grain size numbers in the high temperature heat affected zone (SMAW, 0.7kJ/mm, E307 Electrode)

Number	n	L (cm)	M	N	N from ASTM Eyepiece	Matching grain size (µm)
1	25.1	13	400	5.4	4-5	70-80
2	25.1	12	400	5.1	4-5	70-80
3	25.1	11	400	4.9	4-5	70-80
4	25.1	11	400	4.9	4-5	70-80
Average				5.1		

#### 4.3.3.1 Charpy V-notch testing and results

Five half size Charpy impact test specimens (10mm × 5mm × 55mm) were machined from each of the E309L and E307 welds. Considerable care was taken to direct the V-notch accurately into the coarse grained high temperature heat affected zone. The notch tip was directed parallel to the welding direction. Weld metal failures, parent metal failures and heat affected zone failures were observed. The failures in the grain growth zone of the E309L welds were bright and shiny intergranular fractures, and the crack propagated through the heat affected zone without deviating into the parent metal or the weld metal. The heat affected zone failures in the E307 welds showed deviation into the parent metal in the center of the fracture surface, and the crack appeared to swerve away from the harder heat affected zone into the parent metal, resulting in higher absorbed Charpy impact energy values. Hardness profiles across the two different welds are shown in figure 4.14 and the Charpy impact energy results are shown graphically in figure 4.15. It is evident that, although the E307 weld metal is harder than the E309L, it is still lower than the hardness of the heat affected zone. This suggested that protection of the HAZ by plastic deformation of the weld metal could as a result also occur when E307L is used as filler. The HAZ of the E307

welds has higher Charpy impact energy values, and may be more likely to be protected by plastic deformation of the weld metal and the 3CR12 parent metal.

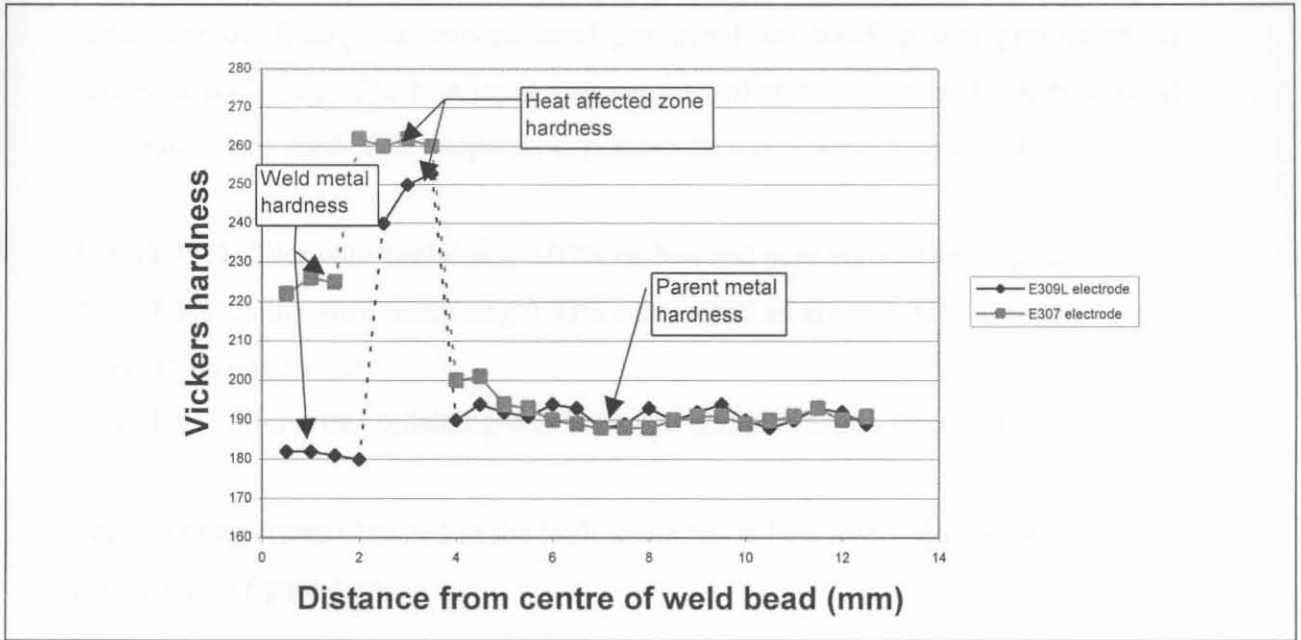


Figure 4.14: Hardness profile for welds in 3CR12 (SMAW, HI = 0.7kJ/mm)

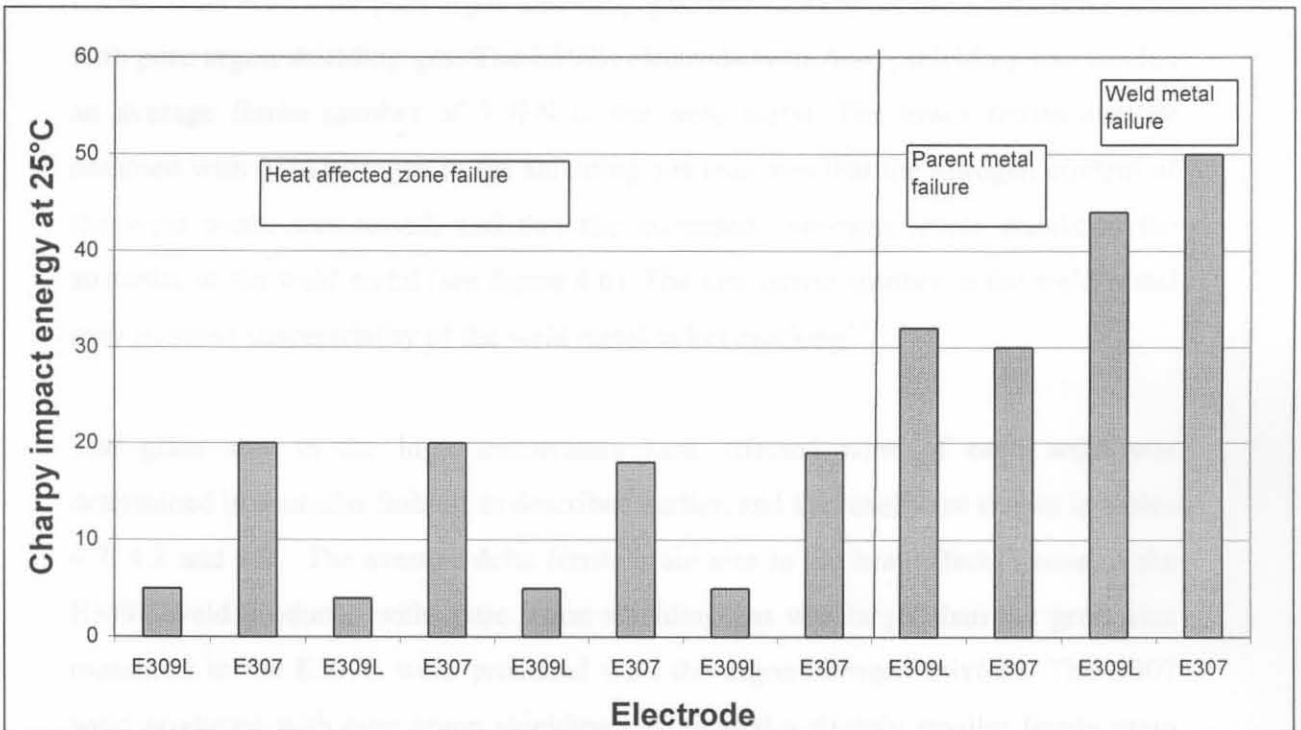


Figure 4.15: Charpy Impact Energy values at 20 °C (SMAW, HI = 0.7kJ/mm)

#### 4.3.4 Gas metal arc welding with E309L (Ar and Ar+N<sub>2</sub>) and E307 (Ar)

In order to investigate the influence of nitrogen additions to the shielding gas, and a higher carbon filler wire, experimental gas metal arc welding was performed on 12mm 3CR12 plate. The heat input was maintained at 1.2kJ/mm and a K-type weld preparation was used. Three separate experimental welds were done namely:

1. An E309L filler wire containing 0.03% carbon and pure argon shielding gas.
2. An E309L filler wire containing 0.03% carbon and an argon + 33% nitrogen shielding gas mixture.
3. An E307 filler wire containing 0.16% carbon and pure argon shielding gas.

The microstructures obtained in the high temperature heat affected zone of each weld are shown in figure 4.16.

The microstructure in the weld metal of each weld consisted of austenite and ferrite. The average ferrite numbers from Fischer Ferritscope readings were 15.1FN for the E309L filler wire with pure argon shielding gas, and 12.8FN for the E 307 filler wire with pure argon shielding gas. The E309L electrode with Ar-N<sub>2</sub> shielding gas yielded an average ferrite number of 5.9FN in the weld metal. The lower ferrite number obtained with 33% nitrogen in the shielding gas indicates that the nitrogen content of the weld metal was raised, and that the increased nitrogen levels stabilized the austenite in the weld metal (see figure 4.6). The low ferrite number in the weld metal may increase susceptibility of the weld metal to hot cracking<sup>12</sup>.

The grain size in the high temperature heat affected zone of each weld was determined in a similar fashion as described earlier, and the results are shown in tables 4.7, 4.8 and 4.9. The average delta ferrite grain size in the heat affected zone of the E309L weld produced with pure argon shielding gas was larger than the grain size measured in the E309L weld produced with the argon-nitrogen mixture. The E307 weld produced with pure argon shielding gas yielded a slightly smaller ferrite grain size in the high temperature heat affected zone compared to the E309L welds.

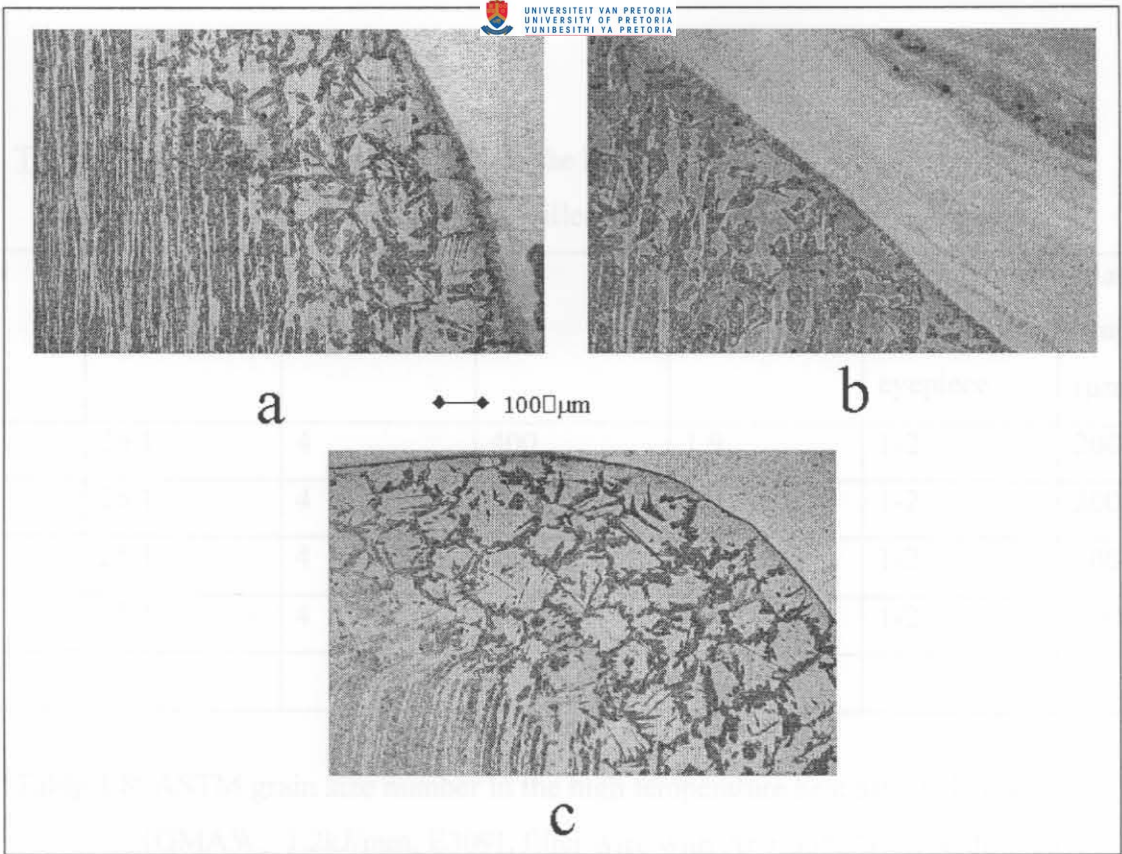


**Figure 4.16:** The microstructure of the weld metal and the heat affected zone in 3CR12 welds. a) E309L + pure argon b)E309L + (Ar + 33%N<sub>2</sub>) c) E307 + pure argon. (GMAW, HI = 1.2kJ/mm, etched by quick swabbing with Kalling's no. 2)

A larger fraction of grain boundary martensite was present in the heat affected zones of the E307 weld (with pure argon) and the E309L weld (with the argon-nitrogen mixture) than in the heat affected zone of the E309L weld (with pure argon shielding gas). Image analysis readings yielded 30% grain boundary martensite in the heat affected zone of the E309L weld (with pure argon), 42.1% grain boundary martensite in the heat affected zone of the E307 weld (with pure argon) and 41% grain boundary martensite in the heat affected zone of the E309L weld (with the argon-nitrogen mixture). The smaller grain size and larger fraction of martensite in the case of E307 and E309L (with Ar-N<sub>2</sub> mixture) suggest that diffusion of interstitial elements across the fusion line into the heat affected zone took place, and that the microstructure of the heat affected zone can be altered to a certain extent by this procedure.



**Table 4.7:** ASTM grain size numbers in the high temperature heat affected zone  
 (GMAW, 1.2kJ/mm, E309L filler wire, pure argon shielding gas)

Number	L (cm)	n	M	N	N from ASTM eyepiece	Matching grain size ( $\mu\text{m}$ )
1	25.1	4	400	1.9	1-2	200-300
2	25.1	4	400	1.9	1-2	200-300
3	25.1	4	400	1.9	1-2	200-300
4	25.1	4	400	1.9	1-2	200-300
Average				1.9		

**Table 4.8:** ASTM grain size number in the high temperature heat affected zone  
 (GMAW, 1.2kJ/mm, E309L filler wire with Ar + 33% N<sub>2</sub> shielding gas)

Number	L (cm)	n	M	N	N from ASTM eyepiece	Matching grain size ( $\mu\text{m}$ )
1	25.1	11	400	4.9	4-5	70-80
2	25.1	10	400	4.6	4-5	70-80
3	25.1	11	400	4.9	4-5	70-80
4	25.1	12	400	5.1	4-5	70-80
Average				4.9		

**Table 4.9:** ASTM grain size numbers in the high temperature heat affected zone  
 (GMAW, 1.2kJ/mm, E307 filler wire, pure argon shielding gas)

Number	L (cm)	n	M	N	N from ASTM eyepiece	Matching grain size ( $\mu\text{m}$ )
1	25.1	13	400	5.4	4-5	70-80
2	25.1	14	400	5.6	4-5	70-80
3	25.1	13	400	5.4	4-5	70-80
4	25.1	12	400	5.1	4-5	70-80
Average				5.4		

#### 4.3.4.1 Charpy V-notch testing and results

Six Charpy impact (10mm × 10mm × 55mm) specimens were prepared from each of the welds. A butter layer K-type preparation was used. The V-notch was carefully directed into the heat-affected zone, parallel to the welding direction. In the E309L weld with the argon-nitrogen mixture and in the E307 weld with the pure argon shielding gas, the crack deviated into the parent metal in the central region of the specimen. In the E309L weld with pure argon shielding gas, the heat affected zone failures appeared bright and intergranular with the crack propagating straight through the grain growth zone without deviation. The facet size corresponded with the grain size observed earlier. Hardness profiles across the three welds are shown in figure 4.17 and the Charpy impact energy results are given in figure 4.18. Figure 4.17 indicates that the hardness of the weld metal of the three welds is approximately the same. The HAZ of the E307 welds is much harder than that of the E309L welds. The E307 HAZ is also more impact resistant as a result of the finer grain structure. The HAZ is more likely to be protected by plastic deformation of the 3CR12 parent metal and the E307 weld metal. As a result, the overall impact resistance of a joint in 3CR12 with an E307 filler would be larger than a joint with an E309L filler.

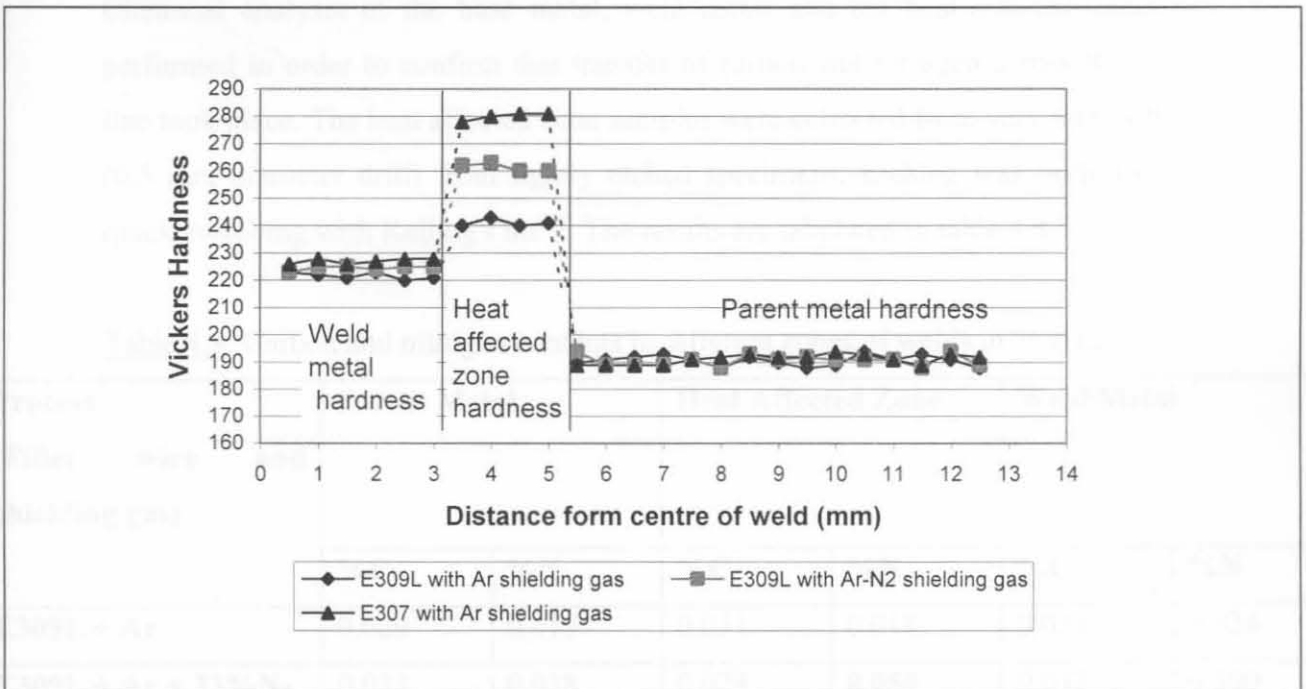


Figure 4.17: Hardness profile for welds in 3CR12 (GMAW, HI = 1.2kJ/mm)

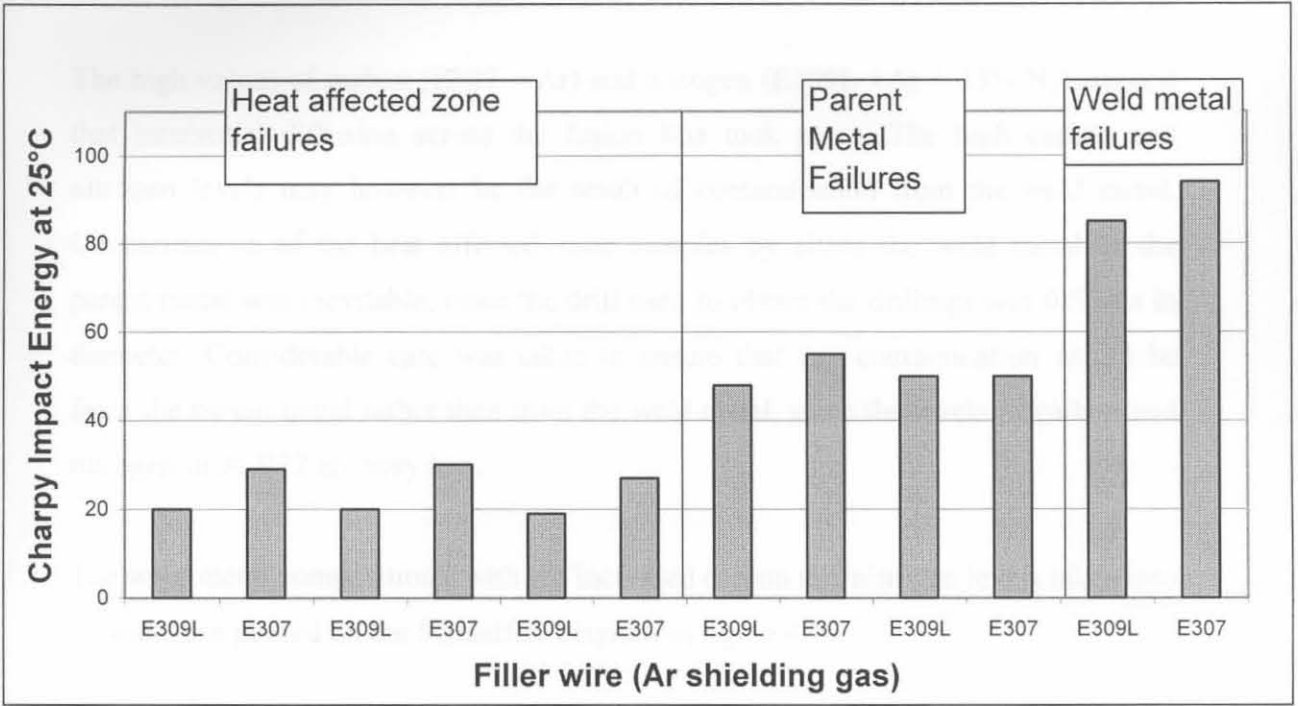


Figure 4.18: Charpy Impact Energy values at 20 C. (GMAW, HI = 1.2kJ/mm)

#### 4.3.4.2 Chemical analysis

Chemical analysis of the base metal, weld metal and the heat-affected zone was performed in order to confirm that transfer of carbon and nitrogen across the fusion line took place. The heat affected zone samples were collected from very fine drillings (0.5 mm diameter drill) from lightly etched specimens. Etching was performed by quick swabbing with Kalling's no. 2. The results are tabulated in table 4.8.

Table 4.8: Carbon and nitrogen contents in different zones of welds in 3CR12.

Process (Filler wire and shielding gas)	Parent Metal		Heat Affected Zone		Weld Metal	
	%C	%N	%C	%N	%C	%N
E309L + Ar	0.029	0.019	0.031	0.018	0.032	0.024
E309L + Ar + 33%N <sub>2</sub>	0.033	0.018	0.028	<b>0.050</b>	0.032	0.500
E307 +Ar	0.027	0.017	<b>0.053</b>	0.019	0.130	0.020

The high values of carbon (E307 + Ar) and nitrogen (E309L + Ar + 33% N<sub>2</sub>) suggest that interstitial diffusion across the fusion line took place. The high carbon and nitrogen levels may however be the result of contamination from the weld metal. Contamination of the heat affected zone samples by either the weld metal or the parent metal was inevitable, since the drill used to obtain the drillings was 0.5 mm in diameter. Considerable care was taken to ensure that any contamination would be from the parent metal rather than from the weld metal, since the levels of carbon and nitrogen in 3CR12 are very low.

The weld metal compositions, with the increased carbon and nitrogen levels taken into account, are plotted on the Schaeffler diagram in figure 4.19.

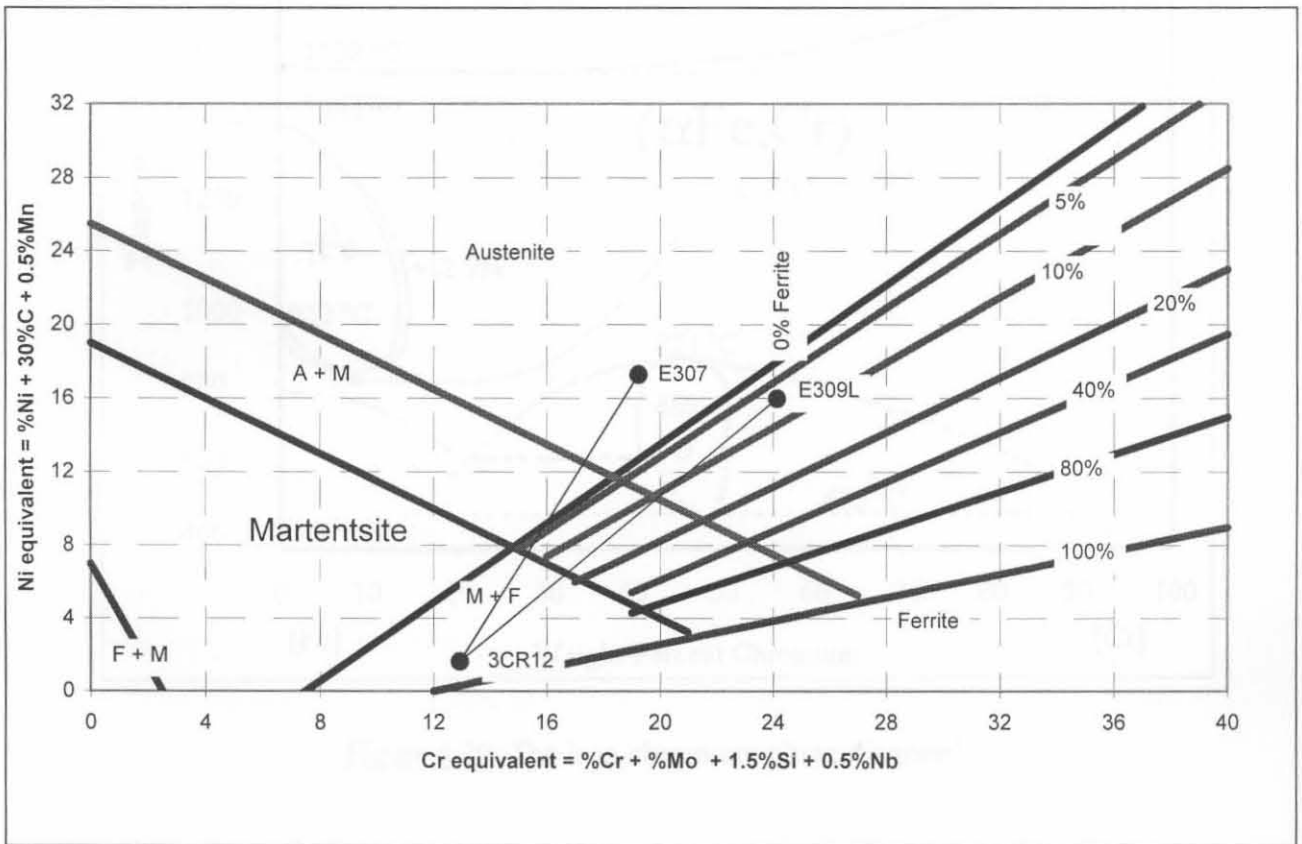


Figure 4.19: The Schaeffler diagram with the two different GMAW experimental welds.

## 4.4 Post weld heat treatment

### 4.4.1 Introduction

As discussed earlier, conventional ferritic stainless steels are subject to grain growth in the heat-affected zone, which leads to low toughness levels in thicker plate sections. The grain size cannot be refined as there is an absence of transformation in these steels because their compositions place them on the right side of the gamma loop on the iron-chromium equilibrium diagram (figure 4.20)<sup>1</sup> A similar problem is experienced during the welding of 3CR12, with the difference that the composition of 3CR12 places it in the region where a dual phase ferritic-austenitic structure can exist

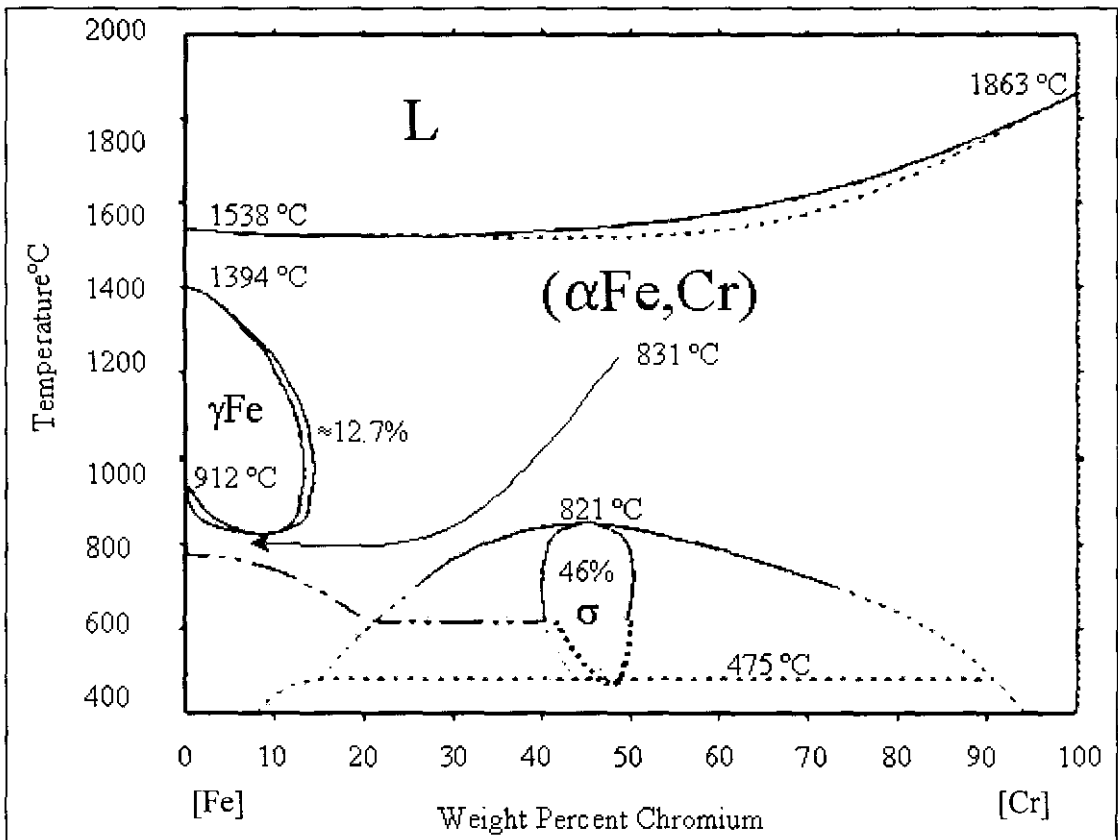


Figure 4.20: The iron-chromium phase diagram<sup>1</sup>.

at elevated temperatures, i.e. in the dual phase region on the extreme right of the loop. During welding, the high temperature heat affected zone, as discussed earlier, is heated through the dual phase region into the delta ferrite phase field, and upon cooling some austenite reforms on the grain boundaries. The grain boundary austenite restricts further delta ferrite grain growth during cooling. As the cooling rate through



the dual phase region after welding is rapid, it is unlikely that all the austenite that would have formed in the dual-phase region during slow cooling would form during welding. This suggests that the microstructure of the HAZ can be altered by heat treatment. Especially in view of the influence of martensite as determined by Zaayman<sup>3</sup> (as discussed earlier), the potential importance of post-weld heat treatment was investigated.

#### 4.4.2. Hardening

In simulation experiments carried out by Zaayman<sup>3</sup>, a decrease in the DBTT's of two different 11% to 12% chromium steels was detected as soon as the martensite content of these steels exceeded 90% after austenitizing at 1000 °C. This occurred in spite of an increase in hardness. The beneficial effect of the finer structure resulting from the formation of martensite exceeded the detrimental effect of increased hardness<sup>3</sup>. Austenitizing the heat affected zone could result in an improvement in the impact properties of the weld, as the large fraction of austenite that exist in the microstructure at elevated temperatures transform to martensite on cooling. This transformation refines the structure.

Most of the carbon in a ferric-martensitic stainless steel segregate to the austenite in the dual-phase region at elevated temperatures. The austenite is normally air hardenable<sup>10</sup> to a large extent, and it can be assumed that the austenite in the high temperature heat affected zone of 3CR12 will transform to martensite upon air cooling. In order to obtain a fully martensitic structure during air cooling, two conditions<sup>10</sup> have to be met:

1. The balance of alloying elements must produce a fully austenitic structure at the austenitizing temperature, e.g. 1050 °C.
2. The  $M_s$  to  $M_f$  temperature range must be above room temperature to eliminate retained austenite.

The  $M_s$  of the austenite in 3CR12 is well above room temperature, and the  $M_s$  to  $M_f$  range is expected to be above room temperature. As a result, all the austenite that formed during the austenitizing heat treatment would probably transform to martensite.

### 4.4.3 Tempering

Based on simulation experiments, Zaayman<sup>3</sup> reported a decrease in DBTT of 70°C and 30°C respectively in two different 11% to 12% chromium steel heats after tempering a 95% and a 100% martensite structure at 750 °C for 1 hour. The beneficial effect of tempering is due to a decrease in hardness of the martensite structure caused by the precipitation and growth of carbides in the martensite matrix. The influence of higher carbon and nitrogen content would be to increase the tempering resistance of the steel, as shown in figure 4.21<sup>1</sup>. The increase in tempering resistance causes the structure to be slightly harder after tempering than a structure with less carbon, but a decrease in hardness still occurs during tempering. The decrease in hardness is sufficient to cause an improvement in the impact properties of the structure. It is expected that tempering would be an appropriate method of improving the fracture toughness of the heat affected zone after hardening. The temper parameter is given by equation (4.5)<sup>1</sup>.

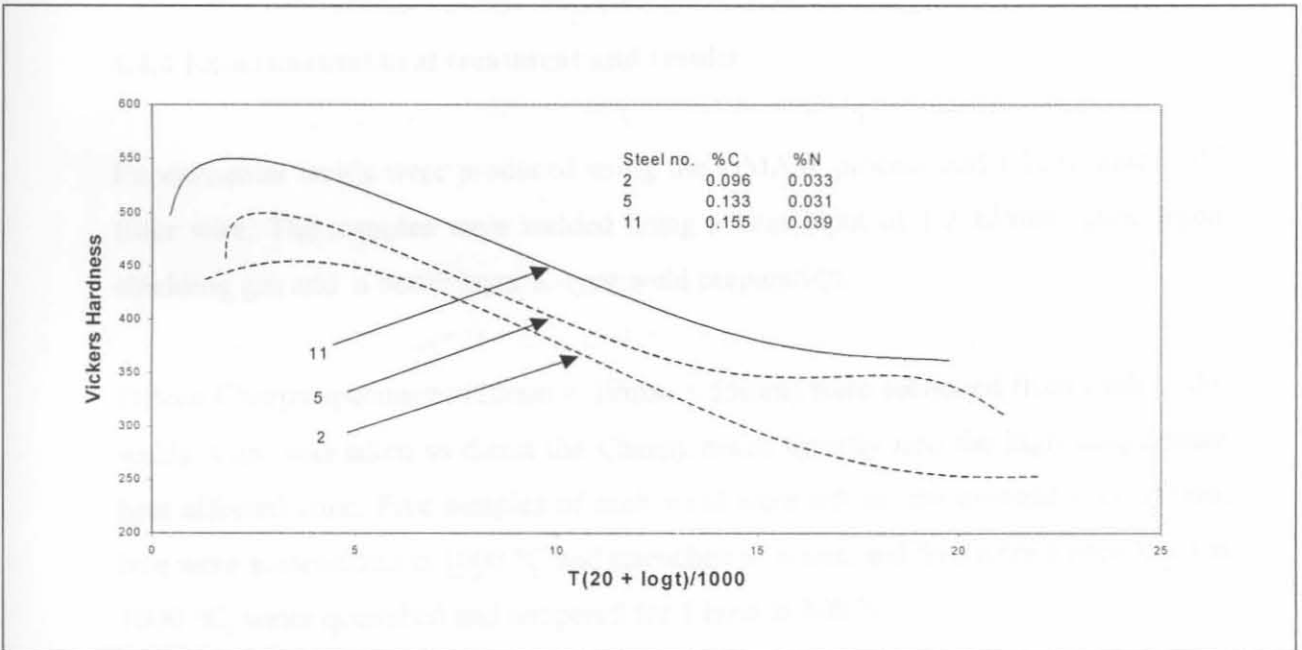


Figure 4.21: The effect of carbon and nitrogen on the tempering of a 12% Cr steel<sup>1</sup>.

$$P = T(k + \log t) \dots\dots\dots(4.5)$$

where P = temper parameter

T = temperature in K

k = constant = 20 for alloy steels<sup>1</sup>

t = time in hours

Temper curves for stainless steels indicate that a temper parameter of about 21 000 is required to decrease the hardness to a value less than 200 DPN during tempering.<sup>1</sup> That would translate into 1050K (777 °C) for 1 hour. If the increase in tempering resistance is taken into account, a temper heat treatment for 1 hour at approximately 800 °C would be reasonable practice to improve the impact strength of the heat affected zone in 3CR12 after hardening. The proposed tempering heat treatment temperature is high: just below the ferrite-to-austenite transformation temperature at approximately 820 °C.

#### 4.4.4 Experimental heat treatment and results

Experimental welds were produced using the GMAW process and E309L and E307 filler wire. The samples were welded using a heat input of 1.2 kJ/mm, pure argon shielding gas and a butter layer K-type weld preparation.

Fifteen Charpy specimens (10mm × 10mm × 55mm) were sectioned from each of the welds. Care was taken to direct the Charpy notch directly into the high temperature heat affected zone. Five samples of each weld were left in the as-welded condition, five were austenitized at 1000 °C and quenched in water, and five were austenitized at 1000 °C, water quenched and tempered for 1 hour at 800 °C.

Image analysis yielded 35% martensite in the heat affected zone of the as-welded E309L welds. After hardening, 80% martensite was recorded. The hardened and tempered samples yielded 82% martensite in the heat affected zone.



The as-welded E307 samples contained 44% martensite in the heat affected zone, and after hardening 87.5% martensite was recorded. The hardened and tempered samples yielded 86% martensite in the heat affected zone.

From the results of the impact tests as shown in figure 4.22 it is evident that the hardening heat treatment caused an improvement in the impact properties of the heat affected zone. Further improvement through tempering was limited to the E307 welds. Tempering did not markedly improve the impact properties of the heat affected zone in the E309L welds. The driving force for carbide precipitation in the heat affected zone of the E307 welds is greater due to the higher carbon content. For this reason, the first stages of tempering may be faster in the heat affected zone of the E309L welds. Post-weld heat treatment did not alter the impact properties of the parent metal or the weld metal of both welds.

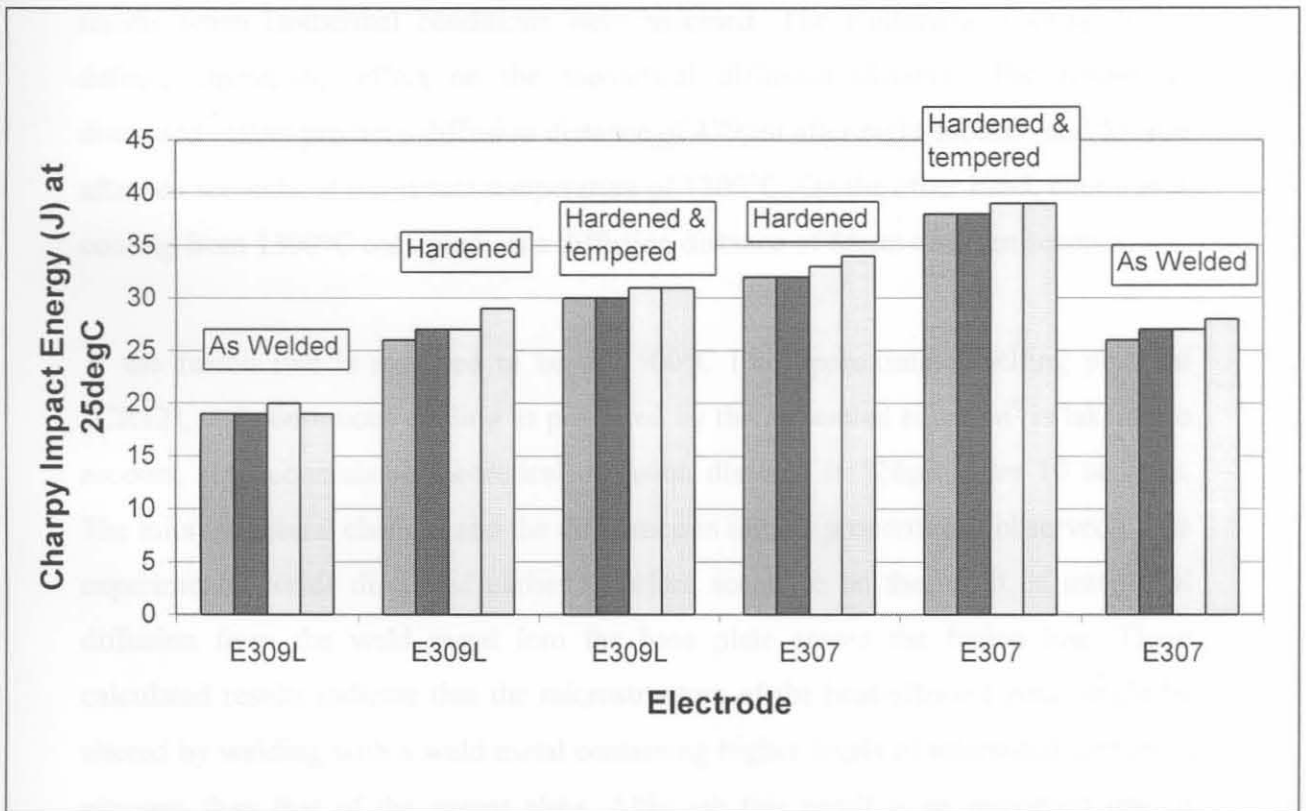


Figure 4.22: Charpy Impact energy values in the heat affected zone at 20 °C.  
(GMAW, HI = 1.3 kJ/mm)

#### 4.5 Continuous cooling and diffusion.

It was mentioned earlier that the isothermal conditions assumed in the diffusion distance calculations were not valid, since the welded plate cools continuously. In order to get a more acceptable model of the interstitial diffusion of carbon during the cooling period of a weld, a temperature sequence for the fusion line (1500°C) of a 1.0 kJ/mm weld in 12mm 3CR12 plate was constructed from the Rosenthal equation<sup>1</sup>. In order to construct the sequence, a period of 40 seconds was divided into time intervals of 0.1 seconds. The diffusion coefficient was calculated at the end of each interval, using the temperature at that time. The average diffusion coefficient was then determined after 1 second, 2 seconds et cetera, up to 10 seconds.

The results of these calculations are shown in figure 4.23, together with the earlier results when isothermal conditions were assumed. The continuous cooling has a definite decreasing effect on the theoretical diffusion distance. The results as discussed earlier predict a diffusion distance of 479µm after eight seconds and 535µm after ten seconds, at a constant temperature of 1300°C. On the other hand, continuous cooling from 1300°C only predicts a diffusion distance of 85µm after ten seconds.

If the fusion line is assumed to be at 1500°C (the approximate melting point of 3CR12), and continuous cooling as predicted by the Rosenthal equation<sup>4</sup> is taken into account, the accumulated theoretical diffusion distance is 326µm after 10 seconds. The microstructural changes and the difference in impact properties as observed in the experimental welds discussed earlier therefore seems to be the result of interstitial diffusion from the weld metal into the base plate across the fusion line. These calculated results indicate that the microstructure of the heat-affected zone might be altered by welding with a weld metal containing higher levels of interstitial carbon or nitrogen than that of the parent plate. Although this result is an important one, it should be mentioned that an increase in carbon might give rise to sensitizing and subsequent loss of corrosion resistance of the 3CR12 parent plate. The aim of this study was however to investigate the possibility of changing the heat affected zone microstructure, and sensitizing behaviour was not investigated.

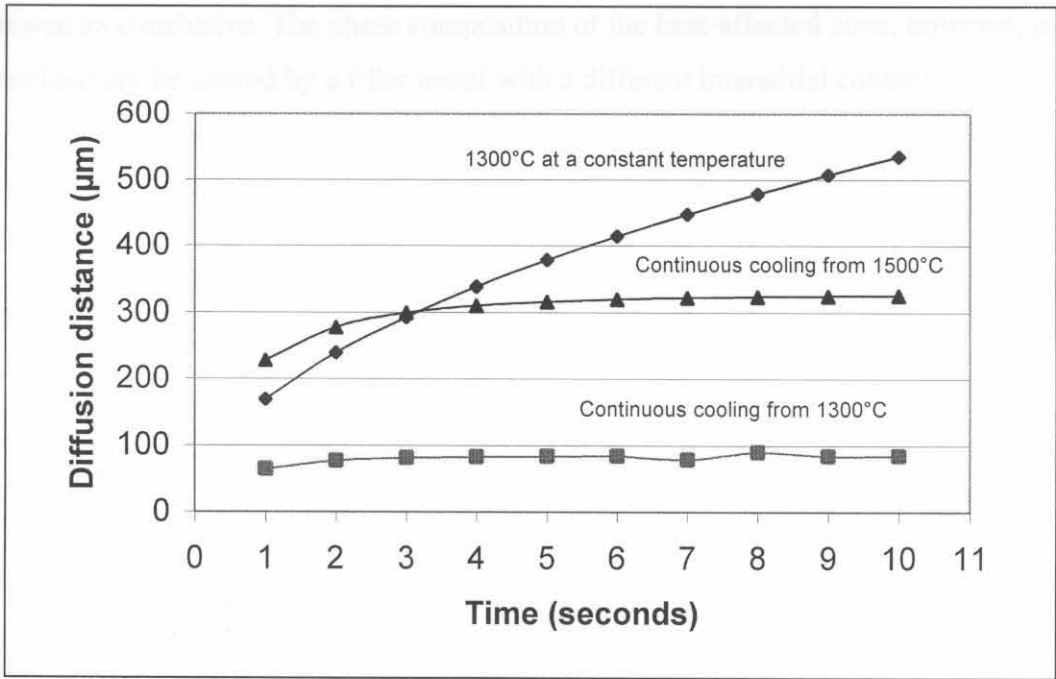


Figure 4.23: Diffusion distance calculated for carbon in 3CR12 for a constant temperature of 1300°C and continuous cooling from 1300°C and 1500°C

#### 4.6 Conclusions

Ferrite grain size in the heat-affected zones of welds in 3CR12 has a detrimental effect on the impact properties of the welded joint. Ferrite grain growth can be inhibited by increasing the high temperature range where austenite is stable. Increasing carbon or nitrogen contents in the heat-affected zone should also increase grain boundary austenite. Consequently, a decrease in ferrite grain growth should be observed in the heat-affected zone of 3CR12 welds.

A decrease in the ferrite grain size occurs in the heat-affected zones of welds in 3CR12 if the carbon or nitrogen content of the weld metal is increased. The finer heat affected zone structure improves the impact properties of the welded joint. Diffusion distance calculations suggest that the finer structure, increase in grain boundary austenite and improvement in impact properties are the result of diffusion of carbon and nitrogen from the weld metal, across the fusion line and into the heat-affected zone. Although an increase in the interstitial content of the heat-affected zone was observed in chemical analysis, contamination of the heat-affected zone samples by the weld metal could not be ruled out. Therefore, the chemical analysis should not be

viewed as conclusive. The phase composition of the heat-affected zone, however, may conclusively be altered by a filler metal with a different interstitial content.

## 4.7 References

1. Llewellyn, D.T.; Steels: Metallurgy and applications; Butterwoth-Heimemann Oxford; Second Edition 1994; Second Impression 1995; pp. 221-262.
2. Easterling, K; Introduction to the physical metallurgy of welding; Butterworth-Heinemann Oxford; Second Edition 1992; Second Impression 1993; pp.1-38.
3. Zaayman, J.J.J.; Improvements to the toughness of the heat affected zone in welds of 11 to 12 per cent chromium steels; Ph.D. UP (1994); pp. 23-101.
3. Grobler, C; Weldability studies on 12% and 14% chromium steels; Ph.D. (UP) (1987); pp. 1- 15.
5. Gooch, T.G & Ginn, T.G; Heat affected zone toughness of MMA welded 12%Cr martensitic- ferritic steels; Report from the co-operative research programme for research members only; The welding institute; Cambridge 1988; pp.1-9.
6. Product Guide for 3CR12; Middelburg Steel and Alloys (Pty) Limited; January 1988; pp. 14-19
7. Stumpf, W.E; Fasetransformasies in die vaste toestand; Kursus op die nagraadse vlak (UP); Uitgawe vir 1995; pp. 307-309.
8. Weertman J. & Weertman J.R.; Elementary Dislocation Theory; The Macmillan Company New York 1964; pp. 1-15
9. Hawkins, D.N, Beech, J & Valtierra-Gallardo, S; A new approach to microstructural control in duplex stainless steel welds; Sheffield; 1988; pp. 199-203.
10. Thelning, K.E; Steel and its heat treatment; Butterworths London; Second Edition 1988; pp. 24-30.

11. Bakker, H et al; Landolt-Börnstein Zahlenwerte und Funktionen aus Naturwissenschaften und Technik; Herausgeber H. Meherer; Band 26; Springer-Verlag Berlin; pp. 481.
12. Kotecki, D.J; (Technical director for stainless and high alloy product development, Lincoln Electric Company Cleveland, Ohio USA); Welding stainless steels; Lecture at the South African Institute of Welding; September 1996.
13. Product Guide for 3CR12; Middelburg Steel and Alloys (Pty) Limited; January 1988; pp. 14-19
14. Holman, J.P.; Heat Transfer; McGraw-Hill Book Company New York 1989; pp. 633-650.